Waves and vibrations in a finitely deformed electroelastic circular cylindrical tube

Luis Dorfmann

Department of Civil and Environmental Engineering
Tufts University, Medford, MA 02155, USA

Ray W. Ogden

School of Mathematics and Statistics, University of Glasgow
Glasgow G12 8SQ, UK

Abstract

In two recent papers, conditions for which axisymmetric incremental bifurcation could arise for a circular cylindrical tube subject to axial extension and radial inflation in the presence of an axial load, internal pressure and a radial electric field were examined, the latter being effected by a potential difference between compliant electrodes on the inner and outer radial surfaces of the tube. The present paper takes this work further by considering the incremental deformations to be time dependent. In particular, both the axisymmetric vibration of a tube of finite length with appropriate end conditions and the propagation of axisymmetric waves in a tube are investigated. General equations and boundary conditions governing the axisymmetric incremental motions are obtained and then, for purposes of numerical evaluation, specialized for a Gent electroelastic model. The resulting system of equations is solved numerically and the results highlight the dependence of the frequency of vibration and wave speed on the tube geometry, applied deformation and electrostatic potential. In particular, the bifurcation results obtained previously are recovered as a special case when the frequency vanishes. Specification of an incremental potential difference in the present work ensures that there is no incremental electric field exterior to the tube. Results are also illustrated for a neo-Hookean electroelastic model and compared with those previously obtained for the case in which no incremental potential difference (or charge) is specified and an external field is required.

1 Introduction

Basic analysis of the finite axisymmetric electroelastic deformation and radial inflation of a circular cylindrical tube of dielectric elastomeric material subject to a radial electric field has been examined by Zhu et al. [1] and Melnikov & Ogden [2] for the situation in which the radial field is generated by a potential difference between thin compliant electrodes on its curved boundaries. An analysis of the stability of the ensuing circular cylindrical configuration based

on the Hessian criterion for a neo-Hookean electroelastic energy function was included in [1], but, as is well known (see [3]), the Hessian criterion does not capture all possible modes of instability. Thus, the more general incremental instability (or bifurcation) analysis was adopted by Melnikov & Ogden [4], based on the general incremental theory developed by Dorfmann & Ogden [5]; see also [6]. They determined possible combinations of axial and radial deformation for which bifurcation could occur for different tube geometries (lengths and radii) and different surface charges in respect of both neo-Hookean and Mooney–Rivlin electroelastic models. Although some of the terms in the general incremental constitutive equations used in [4] were omitted, as pointed out and corrected by Dorfmann & Ogden [7], the results were only marginally affected. In the review [7] corresponding results were obtained for the same neo-Hookean model and also for a Gent electroelastic model. The theory of [5] was also used by Su et al. [8] for the analysis of bifurcation (buckling) of a tube subject to an axial electric field instead of a radial one.

In the present paper we develop the time-dependent counterpart of the incremental analysis in [4, 7], based on the general quasi-electrostatic incremental theory described by Dorfmann & Ogden [9]. Specifically, we consider both axisymmetric vibrations of a tube of finite length with incremental end conditions, and the propagation of axisymmetric waves in an infinitely long tube, the tube being subject to a uniform finite axial extension and a radial inflation accompanied by an internal pressure and a radial electric field. In each case an incremental potential difference between the electrodes is specified, from which it follows that there is no incremental field exterior to the tube, as for the underlying field (whether charge or potential is specified on the electrodes). In the finite deformation context the only related work that we have been able to find in the literature is that by Shmuel & deBotton [10], who analysed axisymmetric waves for the neo-Hookean electroelastic model for a fixed axial stretch or zero axial load. Their method of analysis was different from that adopted here, and, in particular, they accounted for the incremental field exterior to the tube, which is not required in the approach used here.

The content of the present paper is now described briefly. Section 2 summarizes the basic equations of nonlinear electroelasticity, including constitutive equations, equilibrium equations and boundary conditions. In §3 the incremental equations governing the kinematics and motion, together with the boundary conditions and constitutive equations are provided in general form, along with definitions of the electroelastic moduli tensors, including their specialization to the case of an isotropic electroelastic material. The basic equations are applied in §4 to a circular cylindrical tube which is subject to axial extension and radial inflation and a radial electric field generated by a potential difference between compliant electrodes on its inner and outer circular cylindrical boundaries. Then, in §5, the incremental equations from §3 are specialized in order to study axisymmetric electroelastic vibrations and waves in the tube. Lengthy expressions required in this section are relegated to appendices A and B to avoid loss of continuity of the analysis.

Numerical solutions of the resulting system of equations and boundary conditions are then generated in respect of a Gent electroelastic model. In particular, results are provided in graphical form in order to illustrate the dependence of the vibration frequency and wave speed on various geometrical, deformation and electrostatic parameters. When the frequency of vibrations vanishes the results of the bifurcation analysis in [4, 7] are recovered, since the increments are then purely static. In order to compare our results with those in [10], we also illustrate the consequences of the present incremental analysis for a neo-Hookean electroelastic model, and some differences are found because of the different incremental boundary conditions adopted,

but also some similarities, the main focus being on the fundamental mode.

This paper is dedicated to the memory of Professor Peter Chadwick FRS in recognition of his scholarly contributions, especially those to the analysis of elastic waves, and for his support for young scientists working in continuum mechanics.

2 Basic equations

2.1 Kinematics

We begin by setting up a general framework for the static finite deformation of an electroelastic body. We choose a reference configuration, denoted $\mathcal{B}_\mathrm{r}$ with boundary $\partial\mathcal{B}_\mathrm{r}$, in which the body is undeformed and stress free. It is then subject to a finite deformation and an electric field by the action of mechanical and electrical boundary conditions, leading to the configuration $\mathcal{B}$ with boundary $\partial\mathcal{B}$. Let $\mathbf{X}$ be the position vector of a point in $\mathcal{B}_\mathrm{r} \cup \partial\mathcal{B}_\mathrm{r}$, which becomes $\mathbf{x}$ in $\mathcal{B} \cup \partial\mathcal{B}$, and the deformation from $\mathcal{B}_\mathrm{r}$ to $\mathcal{B}$ be represented by the vector function $\boldsymbol{\chi}$, so that $\mathbf{x} = \boldsymbol{\chi}(\mathbf{X})$, it being assumed that $\boldsymbol{\chi}$ has sufficient regularity for the ensuing analysis.

The local deformation, in the neighbourhood of $\mathbf{X}$, is described by the deformation gradient, denoted $\mathbf{F}$, which is defined by

$$\mathbf{F} = \mathrm{Grad}\boldsymbol{\chi}(\mathbf{X}) = \mathrm{Grad}\mathbf{x}, \tag{1}$$

where Grad is the gradient operator with respect to $\mathbf{X}$. The notation $J = \det\mathbf{F} > 0$ will be used, and we note that it connects a volume element $\mathrm{d}v$ in $\mathcal{B}$ to the corresponding volume element $\mathrm{d}V$ in $\mathcal{B}_\mathrm{r}$ according to $\mathrm{d}v = J\mathrm{d}V$, this providing a physical interpretation for J. For an isochoric deformation $J = 1$, and for incompressible materials, on which we mainly focus in this paper, $\mathbf{F}$ satisfies the incompressibility constraint

$$\det\mathbf{F} = 1. \tag{2}$$

If ρ denotes the mass density in $\mathcal{B}$ and ρ_r that in $\mathcal{B}_\mathrm{r}$ then, by mass conservation, they are connected by

$$\rho_\mathrm{r} = J\rho, \tag{3}$$

and, of course, $\rho = \rho_\mathrm{r}$ in the case of incompressibility.

From $\mathbf{F}$ two symmetric and positive definite tensors are defined. These are the left and right Cauchy–Green deformation tensors, given, respectively, by

$$\mathbf{B} = \mathbf{F}\mathbf{F}^\mathrm{T}, \quad \mathbf{C} = \mathbf{F}^\mathrm{T}\mathbf{F}, \tag{4}$$

where the superscript $^\mathrm{T}$ indicates the transpose of a second-order tensor.

2.2 Electrostatics

Let $\mathbf{E}$ and $\mathbf{D}$ denote the electrostatic field and displacement vectors, respectively, in the configuration $\mathcal{B}$. For electrostatics, when there are no free volumetric charges, as for the dielectric materials considered here, the appropriate specialization of Maxwell's equations satisfied by $\mathbf{E}$ and $\mathbf{D}$ are

$$\mathrm{curl}\mathbf{E} = \mathbf{0}, \quad \mathrm{div}\mathbf{D} = 0, \tag{5}$$

where curl and div are the curl and divergence operators with respect to $\mathbf{x}$.

We consider the outside of $\mathcal{B}$ to be a vacuum in which the electric and electric displacement fields are denoted by $\mathbf{E}^\star$ and $\mathbf{D}^\star$, respectively. They are simply connected via the formula $\mathbf{D}^\star = \varepsilon_0 \mathbf{E}^\star$, where ε_0 is the vacuum electric permittivity, and they also satisfy Maxwell's equations (5).

The boundary conditions

$$\mathbf{n} \times (\mathbf{E}^\star - \mathbf{E}) = \mathbf{0}, \quad \mathbf{n} \cdot (\mathbf{D}^\star - \mathbf{D}) = \sigma_{\mathrm{f}} \quad \text{on } \partial\mathcal{B}, \tag{6}$$

have to be satisfied, where $\mathbf{n}$ is the unit outward normal to $\partial\mathcal{B}$ and σ_{f} is the free surface charge per unit area thereon.

For the purposes of developing the constitutive theory and the incremental equations in the following sections it is advantageous to adopt Lagrangian forms of the (Eulerian) field vectors $\mathbf{E}$ and $\mathbf{D}$. These are denoted $\mathbf{E}_{\mathrm{L}}$ and $\mathbf{D}_{\mathrm{L}}$, respectively, and defined, by pulling back from $\mathcal{B}$ to $\mathcal{B}_{\mathrm{r}}$, as

$$\mathbf{E}_{\mathrm{L}} = \mathbf{F}^{\mathrm{T}} \mathbf{E}, \quad \mathbf{D}_{\mathrm{L}} = J \mathbf{F}^{-1} \mathbf{D}. \tag{7}$$

They satisfy the Lagrangian forms of Maxwell's equations

$$\operatorname{Curl} \mathbf{E}_{\mathrm{L}} = \mathbf{0}, \quad \operatorname{Div} \mathbf{D}_{\mathrm{L}} = 0, \tag{8}$$

where Curl and Div are the curl and divergence operators with respect to $\mathbf{X} \in \mathcal{B}_{\mathrm{r}}$.

The boundary conditions (6) are also expressible in Lagrangian form as

$$(\mathbf{F}^{\mathrm{T}} \mathbf{E}^\star - \mathbf{E}_{\mathrm{L}}) \times \mathbf{N} = \mathbf{0}, \quad (J \mathbf{F}^{-1} \mathbf{D}^\star - \mathbf{D}_{\mathrm{L}}) \cdot \mathbf{N} = \sigma_{\mathrm{F}}, \tag{9}$$

where $\mathbf{N}$ is the unit outward normal to $\partial\mathcal{B}_{\mathrm{r}}$, σ_{F} is the free charge density per unit area of $\partial\mathcal{B}_{\mathrm{r}}$, and we point out that as the exterior of $\mathcal{B}_{\mathrm{r}}$ is non-deformable $\mathbf{F}$ is not defined therein and in (9) is evaluated on the boundary from within $\mathcal{B}_{\mathrm{r}}$. The derivation of (9) makes use of Nanson's formula $\mathbf{n}\mathrm{d}a = J \mathbf{F}^{-\mathrm{T}} \mathbf{N} \mathrm{d}A$ connecting area elements $\mathrm{d}A$ and $\mathrm{d}a$ on $\partial\mathcal{B}_{\mathrm{r}}$ and $\partial\mathcal{B}$, respectively; see, for example, standard texts such as [11].

2.3 Stress tensors and equilibrium

Following [12] we adopt the *symmetric total Cauchy stress tensor* $\boldsymbol{\tau}$ for describing the mechanical stress in $\mathcal{B}$, noting that it subsumes the *electrostatic* body forces. Then, when there are no *mechanical* body forces, which we assume to be the case in this paper, the mechanical equilibrium equation has the form

$$\operatorname{div} \boldsymbol{\tau} = \mathbf{0}. \tag{10}$$

There are two main elements when considering traction boundary conditions on the outside of $\partial\mathcal{B}$ associated with (10), namely a possible applied mechanical traction and the traction generated by the external electric field.

Here we write the traction boundary condition in the general form

$$\boldsymbol{\tau} \mathbf{n} = \mathbf{t}_{\mathrm{a}} + \mathbf{t}^\star_{\mathrm{m}} \quad \text{on } \partial\mathcal{B}_{\mathrm{t}}, \tag{11}$$

where $\partial\mathcal{B}_{\mathrm{t}}$ is the part of $\partial\mathcal{B}$ where the mechanical traction $\mathbf{t}_{\mathrm{a}}$ is given, and $\mathbf{t}^\star_{\mathrm{m}} = \boldsymbol{\tau}^\star_{\mathrm{m}} \mathbf{n}$ is the contribution to the traction from the Maxwell stress, denoted $\boldsymbol{\tau}^\star_{\mathrm{m}}$, calculated from the exterior field. The Maxwell stress is defined by

$$\boldsymbol{\tau}^\star_{\mathrm{m}} = \varepsilon_0 \mathbf{E}^\star \otimes \mathbf{E}^\star - \frac{1}{2} \varepsilon_0 (\mathbf{E}^\star \cdot \mathbf{E}^\star) \mathbf{I}, \tag{12}$$

where $\mathbf{I}$ is the identity tensor. Note that $\boldsymbol{\tau}_{\rm m}^{\star}$ satisfies $\operatorname{div}\boldsymbol{\tau}_{\rm m}^{\star}=\mathbf{0}$.

The Lagrangian counterpart of equation (10) is

$$\operatorname{Div}\mathbf{T}=\mathbf{0}, \tag{13}$$

where $\mathbf{T}$ is the *total nominal stress tensor*, which is defined by

$$\mathbf{T}=J\mathbf{F}^{-1}\boldsymbol{\tau}. \tag{14}$$

The traction boundary condition (11) also transforms into Lagrangian form, as

$$\mathbf{T}^{\rm T}\mathbf{N}=\mathbf{t}_{\rm A}+\mathbf{t}_{\rm M}^{\star}\quad\text{on }\partial\mathcal{B}_{\rm rt}, \tag{15}$$

where $\partial\mathcal{B}_{\rm rt}$ is that part of $\partial\mathcal{B}_{\rm r}$ which deforms into $\partial\mathcal{B}_{\rm t}$, $\mathbf{t}_{\rm A}$ is the mechanical traction per unit area of $\partial\mathcal{B}_{\rm r}$ and $\mathbf{t}_{\rm M}^{\star}$ is defined as $\mathbf{t}_{\rm M}^{\star}=\mathbf{T}_{\rm M}^{\star{\rm T}}\mathbf{N}$ on $\partial\mathcal{B}_{\rm r}$, with $\mathbf{T}_{\rm M}^{\star}=J\mathbf{F}^{-1}\boldsymbol{\tau}_{\rm m}^{\star}$.

2.4 Electroelastic constitutive equations

The mechanical and electrostatic fields considered above are linked through electroelastic constitutive equations, which can be used to characterize the properties of electroelastic materials. These are conveniently formulated on the basis of either one of two separate so-called *total energy density functions*. One of these, denoted Ω, depends on the deformation gradient $\mathbf{F}$ and the Lagrangian electric field $\mathbf{E}_{\rm L}$ as independent variables: $\Omega(\mathbf{F},\mathbf{E}_{\rm L})$. The second, denoted Ω^{*}, depends, instead, on $\mathbf{F}$ and the Lagrangian electric displacement field $\mathbf{D}_{\rm L}$: $\Omega^{*}(\mathbf{F},\mathbf{D}_{\rm L})$. They are connected by the partial Legendre transformation

$$\Omega^{*}(\mathbf{F},\mathbf{D}_{\rm L})=\Omega(\mathbf{F},\mathbf{E}_{\rm L})+\mathbf{D}_{\rm L}\cdot\mathbf{E}_{\rm L}, \tag{16}$$

and Ω may be thought of as a complementary energy function relative to the energy function Ω^{*} with respect to the variables $\mathbf{E}_{\rm L}$ and $\mathbf{D}_{\rm L}$.

It should be noted that the superscript * associated with the external fields is distinguished from the asterisk * attached to Ω^{*} and quantities derived therefrom later on related to material properties.

Formulations of the equations based on Ω and Ω^{*} are equivalent, but depending on the problem to be addressed, one may have an advantage over the other. Here, for definiteness, we adopt the formulation based on $\Omega^{*}(\mathbf{F},\mathbf{D}_{\rm L})$, and refer to [12, 6] for details of that based on Ω. From Ω^{*} the total nominal stress tensor, for unconstrained and incompressible materials, respectively, is given by

$$\mathbf{T}=\frac{\partial\Omega^{*}}{\partial\mathbf{F}},\quad \mathbf{T}=\frac{\partial\Omega^{*}}{\partial\mathbf{F}}-p\mathbf{F}^{-1}, \tag{17}$$

where p is a Lagrange multiplier, while in either case, subject to (2) for incompressibility, the Lagrangian electric field is given by

$$\mathbf{E}_{\rm L}=\frac{\partial\Omega^{*}}{\partial\mathbf{D}_{\rm L}}. \tag{18}$$

The corresponding total Cauchy stress and electric field in $\mathcal{B}$ are given by

$$\boldsymbol{\tau}=J^{-1}\mathbf{F}\frac{\partial\Omega^{*}}{\partial\mathbf{F}},\quad \boldsymbol{\tau}=\mathbf{F}\frac{\partial\Omega^{*}}{\partial\mathbf{F}}-p\mathbf{I},\quad \mathbf{E}=\mathbf{F}^{-{\rm T}}\frac{\partial\Omega^{*}}{\partial\mathbf{D}_{\rm L}}. \tag{19}$$

2.4.1 Isotropy

We now specialize the constitutive equations to the case of an isotropic electroelastic material, for which Ω^* is an isotropic function of two tensors, the right Cauchy–Green tensor $\mathbf{C}$, given by $(4)_2$, and $\mathbf{D}_\mathrm{L} \otimes \mathbf{D}_\mathrm{L}$, where $\otimes$ denotes the tensor product. Such a function can be expressed in terms of independent invariants of $\mathbf{C}$ and $\mathbf{D}_\mathrm{L}$. Here, although this choice is far from unique, we choose the principal invariants of $\mathbf{C}$, denoted I_1, I_2, I_3 and defined by

$$I_1 = \mathrm{tr}\mathbf{C}, \quad I_2 = \frac{1}{2}\big[I_1^2 - \mathrm{tr}\big(\mathbf{C}^2\big)\big], \quad I_3 = \det \mathbf{C}, \tag{20}$$

and the $\mathbf{D}_\mathrm{L}$-dependent invariants, denoted I_4, I_5, I_6 and defined by

$$I_4 = \mathbf{D}_\mathrm{L} \cdot \mathbf{D}_\mathrm{L}, \quad I_5 = \mathbf{D}_\mathrm{L} \cdot (\mathbf{C}\mathbf{D}_\mathrm{L}), \quad I_6 = \mathbf{D}_\mathrm{L} \cdot \big(\mathbf{C}^2\mathbf{D}_\mathrm{L}\big). \tag{21}$$

Then Ω^* depends on these invariants and we write $\Omega^* = \bar{\Omega}^*(I_1, I_2, I_3, I_4, I_5, I_6)$ to reflect this, with I_3 omitted in the case of incompressibility.

The stress tensors and the electric field vectors in (17)–(19) can then be expanded out in terms of the invariants. We illustrate this for an incompressible material:

$$\boldsymbol{\tau} = 2\bar{\Omega}_1^*\mathbf{B} + 2\bar{\Omega}_2^*\big(I_1\mathbf{B} - \mathbf{B}^2\big) - p\mathbf{I} + 2\bar{\Omega}_5^*\mathbf{D}\otimes\mathbf{D} + 2\bar{\Omega}_6^*(\mathbf{D}\otimes\mathbf{B}\mathbf{D} + \mathbf{B}\mathbf{D}\otimes\mathbf{D}), \tag{22}$$

$$\mathbf{E} = 2\big(\bar{\Omega}_4^*\mathbf{B}^{-1} + \bar{\Omega}_5^*\mathbf{I} + \bar{\Omega}_6^*\mathbf{B}\big)\mathbf{D}; \tag{23}$$

the shorthand notation $\bar{\Omega}_i^*$ is defined as $\partial\bar{\Omega}^*/\partial I_i$ for $i = 1, 2, 3, 4, 5, 6$ (but with $I_3 = 1$ omitted here). For detailed derivations we refer to [12, 6].

3 Incremental formulation

Superimposed on the basic static configuration $\mathcal{B}$ we now consider a time-dependent incremental deformation and accompanying incremental electric displacement field. These generate incremental stress tensors and an incremental electric field. In the following we discuss the required incremental kinematics, the incremental equations of motion and boundary conditions and incremental constitutive equations, first in general form and then for the case of isotropy.

3.1 Incremental kinematics

Let $\dot{\mathbf{x}} = \dot{\boldsymbol{\chi}}(\mathbf{X}, t)$ denote a time-dependent incremental displacement and the corresponding increment in the deformation gradient by $\dot{\mathbf{F}} = \mathrm{Grad}\dot{\boldsymbol{\chi}}$ superimposed on the configuration $\mathcal{B}$, where a superimposed dot, here and subsequently, signifies an incremental quantity. The Eulerian counterpart of $\dot{\mathbf{x}}$ is denoted $\mathbf{u}(\mathbf{x}, t)$ and is related to $\dot{\mathbf{x}}$ by the identification $\mathbf{u}(\mathbf{x}, t) = \mathbf{u}(\boldsymbol{\chi}(\mathbf{X}, t), t) = \dot{\boldsymbol{\chi}}(\mathbf{X}, t)$.

The increments of $\mathbf{F}$ and related quantities are given by

$$\dot{\mathbf{F}} = \mathbf{L}\mathbf{F}, \quad \dot{J} = J\mathrm{tr}\mathbf{L}, \quad \dot{(\overline{\mathbf{F}^{-1}})} = -\mathbf{F}^{-1}\mathbf{L}, \tag{24}$$

where $\mathbf{L} = \mathrm{grad}\,\mathbf{u}$ is the displacement gradient, grad being the gradient operator with respect to $\mathbf{x}$. For an incompressible material it follows that the incremental form of the incompressibility condition has the form

$$\mathrm{tr}\mathbf{L} \equiv \mathrm{div}\,\mathbf{u} = 0. \tag{25}$$

The incremental velocity and acceleration are $\dot{\mathbf{x}}_{,t} = \mathbf{u}_{,t}$, $\mathbf{v}_{,t} = \dot{\mathbf{x}}_{,tt} = \mathbf{u}_{,tt}$, respectively, where a subscript t following a comma represents $\partial/\partial t$ at fixed material particle $\mathbf{X}$, equivalently at fixed $\mathbf{x}$ since $\mathbf{x} = \boldsymbol{\chi}(\mathbf{X})$ is independent of t.

3.2 Incremental governing equations

3.2.1 Equations of motion

In order to derive the incremental equation of motion we consider briefly the counterpart of the equilibrium equation (13), again in the absence of mechanical body forces, for the situation in which $\mathbf{x}$ depends on time and (13) is replaced by the equation of motion

$$\mathrm{Div}\,\mathbf{T} = \rho_{\mathrm{r}}\mathbf{x}_{,tt}. \tag{26}$$

On taking the increment of both sides of this equation we obtain

$$\mathrm{Div}\,\dot{\mathbf{T}} = \rho_{\mathrm{r}}\dot{\mathbf{x}}_{,tt} = \rho_{\mathrm{r}}\mathbf{u}_{,tt}, \tag{27}$$

where $\dot{\mathbf{T}}$ is the increment in the total nominal stress $\mathbf{T}$.

The corresponding incremental forms of Maxwell's equations (8) are

$$\mathrm{Curl}\,\dot{\mathbf{E}}_{\mathrm{L}} = \mathbf{0}, \quad \mathrm{Div}\,\dot{\mathbf{D}}_{\mathrm{L}} = 0, \tag{28}$$

where $\dot{\mathbf{E}}_{\mathrm{L}}$ and $\dot{\mathbf{D}}_{\mathrm{L}}$ are the increments in $\mathbf{E}_{\mathrm{L}}$ and $\mathbf{D}_{\mathrm{L}}$, respectively.

It is now emphasized that we are considering acousto-electro-elastic waves under the quasi-electrostatic approximation so that the time scales of the mechanical and electromagnetic effects differ to the extent that the time derivatives in the full Maxwell's equations may be neglected, along with the effects of magnetic fields, which do not therefore appear in (28).

The equations coupling the acousto-electro-elastic waves are governed by the three equations in (27) and (28), which require incremental constitutive equations and boundary conditions to complete the picture. Before going on to these it is convenient to update the reference configuration by translating the reference configuration $\mathcal{B}_{\mathrm{r}}$ forward to $\mathcal{B}$. Towards this we denote by $\dot{\mathbf{T}}_0, \dot{\mathbf{D}}_{\mathrm{L}0}, \dot{\mathbf{E}}_{\mathrm{L}0}$ the 'push-forward' versions of $\dot{\mathbf{T}}, \dot{\mathbf{D}}_{\mathrm{L}}, \dot{\mathbf{E}}_{\mathrm{L}}$, respectively, where here and subsequently a subscript 0 indicates a push-forward expression. These are given by

$$\dot{\mathbf{T}}_0 = J^{-1}\mathbf{F}\dot{\mathbf{T}}, \quad \dot{\mathbf{D}}_{\mathrm{L}0} = J^{-1}\mathbf{F}\dot{\mathbf{D}}_{\mathrm{L}}, \quad \dot{\mathbf{E}}_{\mathrm{L}0} = \mathbf{F}^{-\mathrm{T}}\dot{\mathbf{E}}_{\mathrm{L}}, \tag{29}$$

and equations (27) and (28) then translate into the Eulerian forms

$$\mathrm{div}\,\dot{\mathbf{T}}_0 = \rho\mathbf{u}_{,tt}, \quad \mathrm{curl}\,\dot{\mathbf{E}}_{\mathrm{L}0} = \mathbf{0}, \quad \mathrm{div}\,\dot{\mathbf{D}}_{\mathrm{L}0} = 0. \tag{30}$$

3.2.2 Incremental boundary conditions

We now summarize the incremental boundary conditions based on (9) and (15). First, on taking the increments of the electric boundary conditions in (9) and then updating, we obtain

$$(\dot{\mathbf{E}}^{\star} + \mathbf{L}^{\mathrm{T}}\mathbf{E}^{\star} - \dot{\mathbf{E}}_{\mathrm{L}0}) \times \mathbf{n} = \mathbf{0} \quad \text{on} \quad \partial\mathcal{B}, \tag{31}$$

and

$$[\dot{\mathbf{D}}^{\star} + (\mathrm{div}\,\mathbf{u})\mathbf{D}^{\star} - \dot{\mathbf{D}}_{\mathrm{L}0} - \mathbf{L}\mathbf{D}^{\star}] \cdot \mathbf{n} = \dot{\sigma}_{\mathrm{F}0} \quad \text{on} \quad \partial\mathcal{B}, \tag{32}$$

where $\dot{\mathbf{D}}^\star$ and $\dot{\mathbf{E}}^\star$ are the increments of $\mathbf{D}^\star$ and $\mathbf{E}^\star$, respectively, which satisfy the connection $\dot{\mathbf{D}}^\star = \varepsilon_0 \dot{\mathbf{E}}^\star$, while $\dot{\sigma}_{\rm F0}$ is the increment in $\sigma_{\rm F}$ defined per unit area of $\partial\mathcal{B}$. The incremental Maxwell stress is obtained by taking the increment of (12), leading to

$$\dot{\boldsymbol{\tau}}_{\rm m}^\star = \varepsilon_0[\dot{\mathbf{E}}^\star \otimes \mathbf{E}^\star + \mathbf{E}^\star \otimes \dot{\mathbf{E}}^\star - (\mathbf{E}^\star \cdot \dot{\mathbf{E}}^\star)\mathbf{I}], \tag{33}$$

which satisfies $\operatorname{div} \dot{\boldsymbol{\tau}}_{\rm m}^\star = \mathbf{0}$.

Next, on taking the increment of the Lagrangian form of the traction boundary condition (15), we obtain

$$\dot{\mathbf{T}}^{\rm T}\mathbf{N} = \dot{\mathbf{t}}_{\rm A} + J\dot{\boldsymbol{\tau}}_{\rm m}^\star \mathbf{F}^{-{\rm T}}\mathbf{N} - J\boldsymbol{\tau}_{\rm m}^\star \mathbf{F}^{-{\rm T}}\dot{\mathbf{F}}^{\rm T}\mathbf{F}^{-{\rm T}}\mathbf{N} + \dot{J}\boldsymbol{\tau}_{\rm m}^\star \mathbf{F}^{-{\rm T}}\mathbf{N} \quad \text{on} \quad \partial\mathcal{B}_{\rm r}, \tag{34}$$

or, on pushing forward with the help of (24),

$$\dot{\mathbf{T}}_0^{\rm T}\mathbf{n} = \dot{\mathbf{t}}_{\rm A0} + \dot{\boldsymbol{\tau}}_{\rm m}^\star \mathbf{n} - \boldsymbol{\tau}_{\rm m}^\star \mathbf{L}^{\rm T}\mathbf{n} + (\operatorname{div}\mathbf{u})\boldsymbol{\tau}_{\rm m}^\star \mathbf{n} \quad \text{on} \quad \partial\mathcal{B}, \tag{35}$$

where $\dot{\mathbf{t}}_{\rm A0}$ is the incremental mechanical traction per unit area of $\partial\mathcal{B}$.

3.2.3 Incremental constitutive laws

On taking the increments of the two equations in (17) we obtain the linearized equations

$$\dot{\mathbf{T}} = \boldsymbol{\mathcal{A}}^*\dot{\mathbf{F}} + \mathbb{A}^*\dot{\mathbf{D}}_{\rm L}, \quad \dot{\mathbf{T}} = \boldsymbol{\mathcal{A}}^*\dot{\mathbf{F}} + \mathbb{A}^*\dot{\mathbf{D}}_{\rm L} - \dot{p}\mathbf{F}^{-1} + p\mathbf{F}^{-1}\dot{\mathbf{F}}\mathbf{F}^{-1}, \tag{36}$$

for unconstrained and incompressible materials, respectively, and the increment of (18) yields

$$\dot{\mathbf{E}}_{\rm L} = \mathbb{A}^{*{\rm T}}\dot{\mathbf{F}} + \mathsf{A}^*\dot{\mathbf{D}}_{\rm L}, \tag{37}$$

where $\boldsymbol{\mathcal{A}}^*$, $\mathbb{A}^*$ and A^* are, respectively, fourth-, third- and second-order *electroelastic moduli tensors*. In terms of the energy function Ω^* these and the transpose $\mathbb{A}^{*{\rm T}}$ are defined by

$$\boldsymbol{\mathcal{A}}^* = \frac{\partial\Omega^*}{\partial\mathbf{F}\partial\mathbf{F}}, \quad \mathbb{A}^* = \frac{\partial\Omega^*}{\partial\mathbf{F}\partial\mathbf{D}_{\rm L}}, \quad \mathbb{A}^{*{\rm T}} = \frac{\partial\Omega^*}{\partial\mathbf{D}_{\rm L}\partial\mathbf{F}}, \quad \mathsf{A}^* = \frac{\partial\Omega^*}{\mathbf{D}_{\rm L}\partial\mathbf{D}_{\rm L}}. \tag{38}$$

When the Cartesian component forms of vectors and tensors are used, Greek indices are associated with the reference configuration $\mathcal{B}_{\rm r}$ and Roman indices with the configuration $\mathcal{B}$, so that, for example, $\mathbf{F}$ has Cartesian components $F_{i\alpha} = \partial x_i/\partial X_\alpha$, where $i, \alpha \in \{1, 2, 3\}$. The Cartesian components of the moduli tensors are then given by

$$\mathcal{A}^*_{\alpha i\beta j} = \frac{\partial^2\Omega^*}{\partial F_{i\alpha}\partial F_{j\beta}}, \quad \mathbb{A}^*_{\alpha i|\beta} = \frac{\partial^2\Omega^*}{\partial F_{i\alpha}\partial D_{{\rm L}\beta}}, \quad \mathsf{A}^*_{\alpha\beta} = \frac{\partial^2\Omega^*}{\partial D_{{\rm L}\alpha}\partial D_{{\rm L}\beta}}, \tag{39}$$

where the vertical bar in $\mathbb{A}^*_{\alpha i|\beta}$ separates the pair of indices associated with a tensor from the single index associated with a vector, and the products in $(36)_1$ and (37) are given in component form by

$$\dot{T}_{\alpha i} = \mathcal{A}^*_{\alpha i\beta j}\dot{F}_{j\beta} + \mathbb{A}^*_{\alpha i|\beta}\dot{D}_{{\rm L}\beta}, \quad \dot{E}_{{\rm L}_\alpha} = \mathbb{A}^*_{\beta i|\alpha}\dot{F}_{i\beta} + \mathsf{A}^*_{\alpha\beta}\dot{D}_{{\rm L}\beta}. \tag{40}$$

On updating, the incremental constitutive equations (36) and (37) take on the forms

$$\dot{\mathbf{T}}_0 = \boldsymbol{\mathcal{A}}_0^*\mathbf{L} + \mathbb{A}_0^*\dot{\mathbf{D}}_{\rm L0}, \quad \dot{\mathbf{T}}_0 = \boldsymbol{\mathcal{A}}_0^*\mathbf{L} + \mathbb{A}_0^*\dot{\mathbf{D}}_{\rm L0} + p\mathbf{L} - \dot{p}\mathbf{I}, \tag{41}$$

and

$$\dot{\mathbf{E}}_{\rm L0} = \mathbb{A}_0^{*\rm T}\mathbf{L} + \mathbf{A}_0^*\dot{\mathbf{D}}_{\rm L0}, \tag{42}$$

where, in index notation, the push-forward moduli tensors $\boldsymbol{\mathcal{A}}_0^*$, $\mathbb{A}_0^*$, and $\mathbf{A}_0^*$ are defined by

$$\mathcal{A}^*_{0jisk} = J^{-1}F_{j\alpha}F_{s\beta}\mathcal{A}^*_{\alpha i\beta k}, \quad \mathbb{A}^*_{0ji|k} = F_{j\alpha}F^{-1}_{\beta k}\mathbb{A}^*_{\alpha i|\beta}, \quad \mathsf{A}^*_{0ij} = JF^{-1}_{\alpha i}F^{-1}_{\beta j}\mathsf{A}^*_{\alpha\beta}, \tag{43}$$

with $J = 1$ for incompressibility and $\mathbf{u}$ satisfying the incremental incompressibility condition (25).

For later reference we note the symmetries

$$\mathcal{A}^*_{0jisk} = \mathcal{A}^*_{0skji}, \quad \mathbb{A}^*_{0ij|k} = \mathbb{A}^*_{0ji|k}, \quad \mathsf{A}^*_{0ij} = \mathsf{A}^*_{0ji}, \tag{44}$$

and, for an incompressible material, the connections

$$\mathcal{A}^*_{0jisk} - \mathcal{A}^*_{0ijsk} = (\tau_{js} + p\delta_{js})\delta_{ik} - (\tau_{is} + p\delta_{is})\delta_{jk}. \tag{45}$$

between the components of the tensor $\boldsymbol{\mathcal{A}}_0^*$, as given in [5].

For an unconstrained isotropic electroelastic material, $\bar{\Omega}^*$ is a function of the six invariants $I_1, \ldots, I_6$ (five with I_3 omitted for an incompressible material) and the expressions (39) can be expanded in the forms

$$\begin{aligned}
\mathcal{A}^*_{\alpha i\beta j} &= \sum_{m=1,m\neq4}^{6}\sum_{n=1,n\neq4}^{6}\bar{\Omega}^*_{mn}\frac{\partial I_m}{\partial F_{i\alpha}}\frac{\partial I_n}{\partial F_{j\beta}} + \sum_{n=1,n\neq4}^{6}\bar{\Omega}^*_{n}\frac{\partial^2 I_n}{\partial F_{i\alpha}\partial F_{j\beta}},\\
\mathbb{A}^*_{\alpha i|\beta} &= \sum_{m=4}^{6}\sum_{n=1,n\neq4}^{6}\bar{\Omega}^*_{mn}\frac{\partial I_m}{\partial D_{\rm L\beta}}\frac{\partial I_n}{\partial F_{i\alpha}} + \sum_{n=5}^{6}\bar{\Omega}^*_{n}\frac{\partial^2 I_n}{\partial F_{i\alpha}\partial D_{\rm L\beta}},\\
\mathsf{A}^*_{\alpha\beta} &= \sum_{m=4}^{6}\sum_{n=4}^{6}\bar{\Omega}^*_{mn}\frac{\partial I_m}{\partial D_{\rm L\alpha}}\frac{\partial I_n}{\partial D_{\rm L\beta}} + \sum_{n=4}^{6}\bar{\Omega}^*_{n}\frac{\partial^2 I_n}{\partial D_{\rm L\alpha}\partial D_{\rm L\beta}},
\end{aligned} \tag{46}$$

where $\bar{\Omega}^*_n = \partial\bar{\Omega}^*/\partial I_n$, $\bar{\Omega}^*_{mn} = \partial^2\bar{\Omega}^*/\partial I_m\partial I_n$, while their updated counterparts are obtained from (43) but not given separately here. Expressions for the first and second derivatives of I_n, $n = 1, \ldots, 6$ ($n = 1, 2, 4, 5, 6$ for an incompressible material), with respect to $\mathbf{F}$ and $\mathbf{D}_{\rm L}$ are given in [5]; see also Chapter 9 of [6].

In the following sections we apply the foregoing theory to the geometry of a circular cylindrical tube. First, in §4, we provide the equations governing the basic deformation that maintains the circular cylindrical shape of the tube under axial tension and radial inflation for the situation in which the curved boundaries of the tube carry compliant electrodes between which a potential difference is applied. In §5 the equations and boundary conditions governing axisymmetric incremental motions of the tube are derived and in §5.1 these are solved numerically for a simple model electroelastic constitutive law.

4 Equations for a circular cylindrical tube

4.1 Geometry and deformation

Here we first specify the reference geometry of a circular cylindrical tube as having inner and outer radii A and B and length L according to

$$0 < A \leq R \leq B, \quad 0 \leq \Theta \leq 2\pi, \quad -L/2 \leq Z \leq L/2, \tag{47}$$

where (R, Θ, Z) are cylindrical polar coordinates. Affixed to the surfaces $R = A$ and $R = B$ are thin flexible electrodes.

The tube is then deformed along with the flexible electrodes so that its circular cylindrical shape is maintained and, with respect to cylindrical polar coordinates (r, θ, z) its deformed configuration is defined by

$$a \leq r \leq b, \quad 0 \leq \theta \leq 2\pi, \quad -l/2 \leq z \leq l/2, \tag{48}$$

where a and b are its inner and outer deformed radii and l its deformed length, which is given by $l = \lambda_z L$, λ_z being the constant axial stretch. The deformation is achieved by the combination of an internal pressure, an axial load and a potential difference between the electrodes, which generates an electric field that is essentially radial except near the ends of the tube, which are taken to be closed to allow for an internal pressure. Here it is assumed that the L is sufficiently larger than B so that end effects can be neglected.

Because of the form of the deformed geometry the deformation requires that $\theta = \Theta$ and $z = \lambda_z Z$, while for an incompressible material, on which we focus here, the radial component of the deformation is given by

$$r^2 = a^2 + \lambda_z^{-1}(R^2 - A^2), \tag{49}$$

and it follows that

$$b^2 = a^2 + \lambda_z^{-1}(B^2 - A^2), \tag{50}$$

i.e. a and b are not independent when the reference geometry and λ_z are given.

Let $\lambda \equiv r/R$ and λ_r denote the azimuthal and radial stretches, respectively. Then, incompressibility requires that $\lambda_r = \lambda^{-1}\lambda_z^{-1}$. In terms of the independent stretches λ and λ_z the invariants $(20)_{1,2}$ become

$$I_1 = \lambda^2 + \lambda_z^2 + \lambda^{-2}\lambda_z^{-2}, \quad I_2 = \lambda^{-2} + \lambda_z^{-2} + \lambda^2\lambda_z^2. \tag{51}$$

4.2 The electric field

A potential difference is applied between the flexible electrodes on the surfaces $R = A$ and $R = B$ that generates a radial electric component, denoted $E = E(r)$, in the deformed configuration and an associated electric displacement component, denoted $D = D(r)$, with equal and opposite charges, denoted $\pm Q$, on the deformed electrodes. We emphasize that end effects are neglected here and that the electric field is purely radial and dependent only on r. Moreover, by Gauss's theorem, there is no field outside the tube.

Of Maxwell's equations in (5), the first is automatically satisfied, and the second reduces to $\mathrm{d}(rD)/\mathrm{d}r = 0$. Thus, rD is a constant: $rD(r) = aD(a) = bD(b)$. The electric boundary conditions on $r = a$ and $r = b$, obtained by specializing (6) with $\mathbf{E}^\star = \mathbf{D}^\star = \mathbf{0}$, reduce to $D(a) = \sigma_{\mathrm{f}a}, D(b) = -\sigma_{\mathrm{f}b}$, where $\sigma_{\mathrm{f}a}$ and $\sigma_{\mathrm{f}b}$ are the surface charge densities on $r = a$ and $r = b$, respectively. These are given in terms of Q by $\sigma_{\mathrm{f}a} = Q/(2\pi a l), \sigma_{\mathrm{f}b} = -Q/(2\pi b l)$, where $+Q$ (which may be positive or negative) is taken to be the charge on $r = a$.

Let E_{L} and D_{L} denote the Lagrangian counterparts of E and D. Then, for the considered deformation, we obtain from the specialization of (7) the connections $D_{\mathrm{L}} = \lambda_r^{-1} D = \lambda\lambda_z D$ and $E_{\mathrm{L}} = \lambda_r E = \lambda^{-1}\lambda_z^{-1} E$. The invariants (21) are then expressible in the form

$$I_4 = D_{\mathrm{L}}^2, \quad I_5 = \lambda^{-2}\lambda_z^{-2} I_4, \quad I_6 = \lambda^{-4}\lambda_z^{-4} I_4 \tag{52}$$

in terms of three independent variables, namely λ, λ_z and I_4.

4.3 Constitutive specialization and governing equations

For an incompressible isotropic electroelastic material the energy function $\bar{\Omega}^*$ depends on the invariants I_1, I_2, I_4, I_5, I_6, in general. For simplicity we now specialize $\bar{\Omega}^*$ so that it has the simple standard form

$$\bar{\Omega}^*(I_1, I_5) = W(I_1) + \varepsilon^{-1} I_5/2, \tag{53}$$

where $W(I_1)$ is any suitable purely elastic energy function depending only on I_1 and the constant ε is the permittivity of the material. Then, from (22) and (23), the total Cauchy stress tensor and electric field vector take on the simpler forms

$$\boldsymbol{\tau} = 2W_1\mathbf{B} - p\mathbf{I} + \varepsilon^{-1}\mathbf{D}\otimes\mathbf{D}, \quad \mathbf{E} = \varepsilon^{-1}\mathbf{D}. \tag{54}$$

When further specialized to the present geometry, we have

$$\tau_{rr} = 2W_1\lambda_r^2 - p + \varepsilon^{-1}D^2, \quad \tau_{\theta\theta} = 2W_1\lambda^2 - p, \quad \tau_{zz} = 2W_1\lambda_z^2 - p, \tag{55}$$

and $E = \varepsilon^{-1}D$, and hence, on elimination of p, the principal stress differences are obtained as

$$\tau_{\theta\theta} - \tau_{rr} = 2W_1(\lambda^2 - \lambda_r^2) - \varepsilon^{-1}D^2, \quad \tau_{zz} - \tau_{rr} = 2W_1(\lambda_z^2 - \lambda_r^2) - \varepsilon^{-1}D^2. \tag{56}$$

With $D = a\sigma_{\rm fa}/r$ from the previous section and $\operatorname{curl}\mathbf{E} = \mathbf{0}$ yielding $\mathbf{E} = -\operatorname{grad}\phi$, where ϕ is the electrostatic potential, then specialized to $E = -\mathrm{d}\phi/\mathrm{d}r$, integration between a and b gives the potential difference, say V, between the electrodes as

$$V = \varepsilon^{-1}a\sigma_{\rm fa}\log(b/a) = \varepsilon^{-1}Q\log(b/a)/(2\pi l), \tag{57}$$

as in [2, 4]. This expression can be used to translate between results for fixed V and fixed Q.

The equilibrium equation (10) reduces to

$$r\frac{\mathrm{d}\tau_{rr}}{\mathrm{d}r} = \tau_{\theta\theta} - \tau_{rr}, \tag{58}$$

and on the surfaces $r = a$ and $r = b$ there is no Maxwell stress, while, associated with this equation, the mechanical load applied consists of an internal pressure P_a and an external pressure P_b. Thus,

$$\tau_{rr} = -P_a \quad \text{on} \quad r = a, \quad \tau_{rr} = -P_b \quad \text{on} \quad r = b. \tag{59}$$

Integration of (58) with the boundary conditions (59) and the formula (56) yields

$$P(a, Q) \equiv P_a - P_b = 2\int_a^b W_1(\lambda^2 - \lambda_r^2)\frac{\mathrm{d}r}{r} - \frac{1}{2}\varepsilon^{-1}\sigma_{\rm fa}^2(1 - a^2/b^2), \tag{60}$$

which defines the notation $P = P(a, Q)$, with $\sigma_{\rm fa} = Q/(2\pi al)$. Thus P, which may be positive or negative, depends on a and Q when A, B and λ_z are prescribed since b is given by (50). This is equivalent to a formula given in [2], and can alternatively be expressed as a function of a and V on use of (57). When a (equivalently λ_a) and Q (or V) are given then P is determined. It follows that a negative internal pressure is equivalent to an external pressure.

The corresponding expression for the reduced axial load F is [2]

$$F = 2\pi\int_a^b W_1(2\lambda_z^2 - \lambda^2 - \lambda_r^2)r\,\mathrm{d}r - \varepsilon^{-1}\pi a^2\sigma_{\rm fa}^2\log(b/a), \tag{61}$$

and when there is no internal pressure this is the actual axial load.

5 Incremental analysis

We are now concerned with axisymmetric incremental motions so that the incremental displacement $\mathbf{u}$ has cylindrical polar components $u_r, u_\theta = 0, u_z$, with u_r and u_z depending only on r, z and t. The components L_{ij} of the displacement gradient $\mathbf{L}$ are then

$$[L_{ij}] = \begin{bmatrix} u_{r,r} & 0 & u_{r,z} \\ 0 & u_r/r & 0 \\ u_{z,r} & 0 & u_{z,z} \end{bmatrix} \tag{62}$$

and the incremental incompressibility condition (25) reduces to

$$L_{rr} + L_{\theta\theta} + L_{zz} = u_{r,r} + u_r/r + u_{z,z} = 0, \tag{63}$$

where the subscripts r and z following a comma represent partial derivatives. Thus, the components u_r and u_z of $\mathbf{u}$ and $\dot{D}_{\mathrm{L}0r}$ and $\dot{D}_{\mathrm{L}0z}$ of $\dot{\mathbf{D}}_{\mathrm{L}0}$ can be expressed in terms of scalar functions, say ψ and φ, depending on r, z, t, in the form

$$u_r = \frac{\psi_{,z}}{r}, \quad u_z = -\frac{\psi_{,r}}{r}, \quad \dot{D}_{\mathrm{L}0r} = \frac{\varphi_{,z}}{r}, \quad \dot{D}_{\mathrm{L}0z} = -\frac{\varphi_{,r}}{r}, \tag{64}$$

so that $\mathrm{div}\,\mathbf{u} = 0$ and $\mathrm{div}\,\dot{\mathbf{D}}_{\mathrm{L}0} = 0$ are automatically satisfied and it remains to satisfy the two equations $(30)_{1,2}$.

With reference to the cylindrical polar coordinates the relevant components of $\dot{\mathbf{T}}_0$ for a tube under axisymmetric increments are, on use of the incompressibility condition (63) to eliminate $L_{\theta\theta}$,

$$\begin{aligned}
\dot{T}_{0rr} &= (\mathcal{A}^*_{0rrrr} - \mathcal{A}^*_{0rr\theta\theta} + p)L_{rr} + (\mathcal{A}^*_{0rrzz} - \mathcal{A}^*_{0rr\theta\theta})L_{zz} - \dot{p} + \mathbb{A}^*_{0rr|r}\dot{D}_{\mathrm{L}0r}, \\
\dot{T}_{0\theta\theta} &= (\mathcal{A}^*_{0rr\theta\theta} - \mathcal{A}^*_{0\theta\theta\theta\theta} - p)L_{rr} + (\mathcal{A}^*_{0\theta\theta zz} - \mathcal{A}^*_{0\theta\theta\theta\theta} - p)L_{zz} - \dot{p} + \mathbb{A}^*_{0\theta\theta|r}\dot{D}_{\mathrm{L}0r}, \\
\dot{T}_{0zz} &= (\mathcal{A}^*_{0rrzz} - \mathcal{A}^*_{0\theta\theta zz})L_{rr} + (\mathcal{A}^*_{0zzzz} - \mathcal{A}^*_{0\theta\theta zz} + p)L_{zz} - \dot{p} + \mathbb{A}^*_{0zz|r}\dot{D}_{\mathrm{L}0r}, \\
\dot{T}_{0rz} &= \mathcal{A}^*_{0rzrz}L_{zr} + (\mathcal{A}^*_{0rzzr} + p)L_{rz} + \mathbb{A}^*_{0zr|z}\dot{D}_{\mathrm{L}0z}, \\
\dot{T}_{0zr} &= \mathcal{A}^*_{0zrzr}L_{rz} + (\mathcal{A}^*_{0rzzr} + p)L_{zr} + \mathbb{A}^*_{0zr|z}\dot{D}_{\mathrm{L}0z},
\end{aligned} \tag{65}$$

the components of the moduli tensors in general depending on r. The corresponding components of the incremental electric field are given by

$$\begin{aligned}
\dot{E}_{\mathrm{L}0r} &= (\mathbb{A}^*_{0rr|r} - \mathbb{A}^*_{0\theta\theta|r})L_{rr} + (\mathbb{A}^*_{0zz|r} - \mathbb{A}^*_{0\theta\theta|r})L_{zz} + \mathsf{A}^*_{0rr}\dot{D}_{\mathrm{L}0r}, \\
\dot{E}_{\mathrm{L}0z} &= \mathbb{A}^*_{0zr|z}(L_{zr} + L_{rz}) + \mathsf{A}^*_{0zz}\dot{D}_{\mathrm{L}0z}.
\end{aligned} \tag{66}$$

The components of the moduli tensors appearing in (65) and (66) are the only non-zero ones for the considered deformation and single field component, and are independent of the particular choice of (incompressible, isotropic) energy function $\bar{\Omega}^*$. Full expressions for the general isotropic case are given in, for example, [6]. Note that the final term on the right-hand side of $(65)_4$ and the L_{zr} term on the right-hand side of (66) were missing from the corresponding expressions in [4], as already pointed out in [7], although the effect of the omission on the final results is marginal.

From $(30)_1$ the components of the incremental equation of motion are obtained as

$$\dot{T}_{0rr,r} + \frac{1}{r}(\dot{T}_{0rr} - \dot{T}_{0\theta\theta}) + \dot{T}_{0zr,z} = \rho u_{r,tt}, \quad \dot{T}_{0rz,r} + \frac{1}{r}\dot{T}_{0rz} + \dot{T}_{0zz,z} = \rho u_{z,tt}, \tag{67}$$

while $(30)_2$ specialises to

$$\dot{E}_{\mathrm{L}0r,z} - \dot{E}_{\mathrm{L}0z,r} = 0. \tag{68}$$

In order to make the resulting equations relatively compact we introduce the notations defined by

$$a = \mathcal{A}^*_{0zrzr}, \quad 2b = \mathcal{A}^*_{0rrrr} + \mathcal{A}^*_{0zzzz} - 2\mathcal{A}^*_{0rrzz} - 2\mathcal{A}^*_{0rzzr}, \quad c = \mathcal{A}^*_{0rzrz}, \tag{69}$$

$$d = \mathbb{A}^*_{0zr|z}, \quad e = \mathbb{A}^*_{0rr|r} - \mathbb{A}^*_{0zz|r} - d, \quad f = \mathsf{A}^*_{0zz}, \quad g = \mathsf{A}^*_{0rr}, \tag{70}$$

$$h = 2\mathcal{A}^*_{0rrzz} - 2\mathcal{A}^*_{0\theta\theta zz} + \mathcal{A}^*_{0\theta\theta\theta\theta} - \mathcal{A}^*_{0rrrr}, \quad j = \mathbb{A}^*_{0zz|r} - \mathbb{A}^*_{0\theta\theta|r}, \tag{71}$$

$$k = \mathcal{A}^*_{0rrrr} - \mathcal{A}^*_{0rrzz} + \mathcal{A}^*_{0\theta\theta zz} - \mathcal{A}^*_{0rr\theta\theta} - \mathcal{A}^*_{0rzzr}. \tag{72}$$

Then, substitution from (66) into (68) with (62) and (64), followed by substitution from (65) into (67) with (62) and (64) after elimination of $\dot{p}$, yields two coupled equations for ψ and ϕ, namely

$$\begin{aligned} &dr^2\psi_{,rrr} + (rd' - 2d)(r\psi_{,rr} - \psi_{,r}) + er^2\psi_{,rzz} - (rd' + e + j)r\psi_{,zz} \\ &+ fr^2\varphi_{,rr} + (rf' - f)r\varphi_{,r} + gr^2\varphi_{,zz} = 0, \end{aligned} \tag{73}$$

and

$$\begin{aligned} &cr^3\psi_{,rrrr} + 2br^3\psi_{,rrzz} + ar^3\psi_{,zzzz} + 2(rc' - c)r^2\psi_{,rrr} + 2(rb' - b)r^2\psi_{,rzz} \\ &+ (r^2c'' - 3rc' + 3c)(r\psi_{,rr} - \psi_{,r}) - (h + rk' + r^2c'' - r^2\tau''_{rr})r\psi_{,zz} \\ &+ er^3\varphi_{,rzz} + dr^3\varphi_{,rrr} + (re' + rd' + j)r^2\varphi_{,zz} + (2rd' - d)r^2\varphi_{,rr} \\ &+ (r^2d'' - rd')r\varphi_{,r} = \rho r^2(r\psi_{,zz} + r\psi_{,rr} - \psi_{,r})_{,tt}, \end{aligned} \tag{74}$$

in which a prime indicates differentiation with respect to r.

The boundary conditions on $r = a$ and $r = b$ associated with the equations (73) and (74) are now derived. First, the specialisation of (31) with no external field is $\dot{E}_{\mathrm{L}0z} = 0$ on $r = a, b$, which corresponds to a constant incremental potential on $r = a$ and $r = b$, and from $(66)_1$ with (62) and (64) this yields

$$d(r\psi_{,zz} - r\psi_{,rr} + \psi_{,r}) - fr\varphi_{,r} = 0 \quad \text{on} \quad r = a, b. \tag{75}$$

A specified incremental voltage (potential difference) is associated with equal and opposite incremental charges on the electrodes, as can easily be shown by taking the increment of (57), and hence the incremental version of Gauss's theorem implies that there is no incremental field outside the tube, as for the underlying field. From the solution of the incremental equations, the boundary condition (32) then determines the incremental charge, which cannot be specified independently of the incremental potential. Alternatively, the incremental charge can be specified and the roles of the incremental electric and electric displacement boundary conditions can be interchanged. Here, for definiteness, we consider only specification of the incremental potential difference.

The second and third boundary conditions are obtained from the expression (35) for the incremental traction specialised with no external field and $\dot{\mathbf{t}}_{\mathrm{A}0} = P\mathbf{L}^{\mathrm{T}}\mathbf{n}$ for loading with pressure P (P_a or P_b, as appropriate). The only non-trivial components of this yield

$$\dot{T}_{0rz} = P_aL_{rz}, \quad \dot{T}_{0rr} = P_aL_{rr} \quad \text{on} \quad r = a, \quad \dot{T}_{0rz} = P_bL_{rz}, \quad \dot{T}_{0rr} = P_bL_{rr} \quad \text{on} \quad r = b. \tag{76}$$

Note that since there is no underlying external field, $\mathbf{E}^\star = \mathbf{0}$ and hence there is no Maxwell stress and from (33) the incremental Maxwell stress also vanishes. Then, from $(65)_3$ with (62), (64) and the connections $\tau_{rr} = -P_a$ on $r = a$, $\tau_{rr} = -P_b$ on $r = b$ from (59), we then obtain, for the component $\dot{T}_{0rz}$,

$$c(r\psi_{,zz} - r\psi_{,rr} + \psi_{,r}) - dr\varphi_{,r} = 0 \quad \text{on} \quad r = a, b. \tag{77}$$

The combination of (75) and (77) gives the simple pair of boundary conditions

$$r\psi_{,zz} - r\psi_{,rr} + \psi_{,r} = 0, \quad \varphi_{,r} = 0 \quad \text{on} \quad r = a, b, \tag{78}$$

provided $cf - d^2 \neq 0$, which is the case except for trivial forms of energy function and holds for the model considered below.

We emphasize that is easy to show that just as there is no underlying field outside the tube there is no incremental field, as required by the incremental counterpart of Gauss's theorem, whether there is an imposed increment in change or voltage. In [10] an external incremental field was included in the analysis and there was no counterpart of the expression for the incremental Maxwell stress.

For the boundary condition involving $\dot{T}_{0rr}$ the expression $(65)_1$ is first differentiated with respect to z and then $\dot{p}_{,z}$ is eliminated by use of its expression obtained from $(67)_2$ with $(65)_{3,4}$, (62) and (64). After some rearrangements and use of (78) this yields

$$\begin{aligned} &cr^2\psi_{,rrr} + (2b + c)r^2\psi_{,rzz} - (k + 2c - r\tau'_{rr})r\psi_{,zz} \\ &+(d + e)r^2\varphi_{,zz} + dr^2\varphi_{,rr} = \rho r^2\psi_{,rtt} \quad \text{on} \quad r = a, b. \end{aligned} \tag{79}$$

The expression for τ'_{rr} herein can be obtained by using the equilibrium equation (58) in the form $r\tau'_{rr} = \tau_{\theta\theta} - \tau_{rr}$ and that for τ''_{rr} in (74) then follows.

The equations (73) and (74) with the boundary conditions (78) and (79) apply independently of the form of the energy function $\bar{\Omega}^*$ adopted, but for illustrative purposes we now simplify the equations and boundary conditions and the notations therein by specializing to an energy function of the form (53), for which the general component expressions for the moduli are given by

$$\mathcal{A}^*_{0piqj} = 4W_{11}B_{ip}B_{jq} + 2W_1\delta_{ij}B_{pq} + \varepsilon^{-1}\delta_{ij}D_pD_q, \tag{80}$$

$$\mathbb{A}^*_{0pi|q} = \varepsilon^{-1}(\delta_{pq}D_i + \delta_{iq}D_p), \quad \mathsf{A}^*_{0ij} = \varepsilon^{-1}\delta_{ij}. \tag{81}$$

We then have $\mathcal{A}^*_{0rzzr} = 0, \mathbb{A}^*_{0zz|r} = \mathbb{A}^*_{0\theta\theta|r} = 0$ and, in the reduced notation (69)–(72),

$$a = 2W_1\lambda_z^2, \quad 2b = 4W_{11}(\lambda_z^2 - \lambda_r^2)^2 + 2W_1(\lambda_z^2 + \lambda_r^2) + dD, \tag{82}$$

$$c = 2W_1\lambda_r^2 + dD, \quad e = d = \varepsilon^{-1}D, \quad f = g = \varepsilon^{-1} \tag{83}$$

$$h = 4W_{11}\lambda_r^4(1 - \lambda^4\lambda_z^2)(2\lambda^2\lambda_z^4 - \lambda^4\lambda_z^2 - 1) - 2W_1\lambda_r^2(1 - \lambda^4\lambda_z^2) - dD, \tag{84}$$

$$j = 0, \quad k = 4W_{11}\lambda_r^4(1 - \lambda^2\lambda_z^4)(1 - \lambda^4\lambda_z^2) + 2W_1\lambda_r^2 + dD, \tag{85}$$

wherein the notations $W_1 = \mathrm{d}W/\mathrm{d}I_1$, $W_{11} = \mathrm{d}^2W/\mathrm{d}I_1^2$ are adopted, while the corresponding third derivative W_{111} will also be needed later. We also have

$$r\tau'_{rr} = \tau_{\theta\theta} - \tau_{rr} = 2W_1\lambda_r^2(\lambda^4\lambda_z^2 - 1) - dD. \tag{86}$$

We require expressions for $r^2\tau''_{rr}$, rc', r^2c'', rb' and rk', which are fairly lengthy and given in appendix A. We also note that $rd' = -d$ and $r^2d'' = 2d$.

To solve the system of equations and boundary conditions we consider ψ and φ to have the forms

$$\psi(r,z,t) = f_\alpha(r)\cos\alpha z\cos\omega t \quad \text{and} \quad \varphi(r,z,t) = g_\alpha(r)\cos\alpha z\cos\omega t, \tag{87}$$

where ω is the frequency and α is a constant, which is fixed by, for example, setting to zero the radial incremental displacement and normal incremental traction on the ends of the deformed tube, i.e. $u_r = 0$ and $\dot{T}_{0zz} = 0$, which gives

$$\alpha = 2n\pi/l = 2n\pi/(\lambda_z L), \tag{88}$$

where $n = 1, 2, 3, \ldots$ is the mode number of the incremental solutions.

Alternatively, by setting to zero the incremental axial displacement and incremental shear stress, i.e. $u_z = 0$ and $\dot{T}_{0zr} = 0$, we obtain

$$\alpha = (2n+1)\pi/l = (2n+1)\pi/(\lambda_z L), \tag{89}$$

and by replacing $\cos\alpha z$ by $\sin\alpha z$ these boundary conditions can be reversed.

Equation (73) then specializes to

$$D[r^2 f''''_\alpha - 3rf'''_\alpha + (3-\alpha^2r^2)f'_\alpha] + r^2g''_\alpha - rg'_\alpha - \alpha^2r^2g_\alpha = 0 \tag{90}$$

and equation (74) to

$$\begin{aligned} &cr^3 f''''_\alpha + 2(rc'-c)r^2f'''_\alpha + (\rho\omega^2 - 2b\alpha^2)r^3f''_\alpha + (r^2c'' - 3rc' + 3c)(rf''_\alpha - f'_\alpha) \\ &- [2\alpha^2r^2(rb'-b) + \rho\omega^2r^2]f'_\alpha + (a\alpha^2r^2 - \rho\omega^2r^2 + h + rk' + r^2c'' - r^2\tau''_{rr})\alpha^2rf_\alpha \\ &+ d[r^3g'''_\alpha - 3r^2g''_\alpha + (3-\alpha^2r^2)rg'_\alpha + 2\alpha^2r^2g_\alpha] = 0. \end{aligned} \tag{91}$$

The boundary conditions (78) become

$$rf''_\alpha - f'_\alpha + \alpha^2rf_\alpha = 0, \quad g'_\alpha = 0 \quad \text{on} \quad r = a, b \tag{92}$$

and (79) reduces to

$$\begin{aligned} cr^2f'''_\alpha + [\rho\omega^2r^2 - (2b+c)\alpha^2r^2]f'_\alpha + (k + 2c - r\tau'_{rr})\alpha^2rf_\alpha \\ + d(r^2g''_\alpha - 2\alpha^2r^2g_\alpha) = 0 \quad \text{on} \quad r = a, b. \end{aligned} \tag{93}$$

If an infinitely long cylinder is considered then it is appropriate to consider the propagation of waves along the cylinder of the form

$$\psi(r,z,t) = f_\alpha(r)\cos(\alpha z - \omega t) \quad \text{and} \quad \varphi(r,z,t) = g_\alpha(r)\cos(\alpha z - \omega t), \tag{94}$$

with $\omega = \alpha v$, v the wave speed and α the wave number, wherein $\cos$ may be replaced by $\sin$. The equations and boundary conditions on $r = a, b$ remain in force with the change $\omega = \alpha v$, so that the wave speed can be determined in terms of α, which is now the wave number independent of L, and the other parameters in the model.

For either vibrations or waves we follow the procedure used in [7] and arrange the equations as a first-order system in the form

$$\mathbf{y}' = \boldsymbol{\mathcal{M}}\mathbf{y}, \tag{95}$$

where $\mathbf{y} = (y_1, y_2, y_3, y_4, y_5, y_6)$, with $y_1 = f_\alpha, y_2 = y_1', y_3 = y_2', y_4 = y_3', y_5 = g_\alpha, y_6 = y_5'$, a prime indicating differentiation with respect to r, and $\boldsymbol{\mathcal{M}}$ is the 6×6 matrix

$$\boldsymbol{\mathcal{M}} = \begin{bmatrix} 0 & 1 & 0 & 0 & 0 & 0 \\ 0 & 0 & 1 & 0 & 0 & 0 \\ 0 & 0 & 0 & 1 & 0 & 0 \\ M_{41} & M_{42} & M_{43} & M_{44} & 0 & 0 \\ 0 & 0 & 0 & 0 & 0 & 1 \\ 0 & M_{62} & M_{63} & M_{64} & M_{65} & M_{66} \end{bmatrix}, \tag{96}$$

whose non-zero elements M_{4i}, $i \in \{1, \ldots, 4\}$, are quite lengthy and therefore listed in appendix B, while M_{6i}, $i \in \{2, \ldots, 6\}$, are given by

$$M_{62} = (\alpha^2 r^2 - 3)D/r^2, \quad M_{63} = 3D/r, \quad M_{64} = -D, \quad M_{65} = \alpha^2, \quad M_{66} = 1/r. \tag{97}$$

Note that M_{44} and M_{6i}, $i \in \{2, \ldots, 6\}$, are the same as for the static bifurcation problem in [7], but M_{41}, M_{42}, M_{43} are different by virtue of inclusion of the term $\rho\omega^2$.

The corresponding boundary conditions (78) and (79) become, respectively,

$$\alpha^2 r y_1 - y_2 + r y_3 = 0, \quad y_6 = 0, \quad \sum_{i=1}^{6} b_i y_i = 0 \quad \text{on} \quad r = a, b, \tag{98}$$

where the coefficients b_i, $i = 1, \ldots, 6$, are given by

$$b_1 = 2\alpha^2 r[2W_{11}\lambda_r^4(\lambda^4\lambda_z^2 - 1)(\lambda^2\lambda_z^4 - 1) + W_1\lambda_r^2(4 - \lambda^4\lambda_z^2) + 2dD], \tag{99}$$

$$b_2 = -3dD + \rho\omega^2 r^2 - \alpha^2 r^2[4W_{11}\lambda_r^4(\lambda^2\lambda_z^4 - 1)^2 + 2W_1\lambda_r^2(\lambda^2\lambda_z^4 + 2) + dD], \tag{100}$$

$$b_3 = 3dDr, \quad b_4 = 2W_1\lambda_r^2 r^2, \quad b_5 = -d\alpha^2 r^2, \quad b_6 = dr, \tag{101}$$

and we note that the term $\rho\omega^2$ appears only in b_2, which is therefore the only term that differs from the corresponding terms in [7].

In order to illustrate the solution of the above system we specialize the model (53) so that $W(I_1)$ takes on the Gent form [13]

$$W(I_1) = -\frac{1}{2}\mu G \log[1 - (I_1 - 3)/G], \tag{102}$$

where the constant μ is the shear modulus in the reference configuration, G is a non-dimensional material constant, known as the Gent constant. Then, $\bar{\Omega}^*$ becomes

$$\bar{\Omega}^*(I_1, I_5) = -\frac{1}{2}\mu G \log[1 - (I_1 - 3)/G] + \frac{1}{2}\varepsilon^{-1} I_5. \tag{103}$$

The derivatives of the first three derivatives of $W(I_1)$, given by

$$W_1 = \frac{1}{2}\frac{\mu G}{3 + G - I_1}, \quad W_{11} = \frac{1}{2}\frac{\mu G}{(3 + G - I_1)^2}, \quad W_{111} = \frac{\mu G}{(3 + G - I_1)^3}, \tag{104}$$

are required in the formulas for the coefficients in equation (91) and the boundary condition (93) given in appendix A.

In the limit as $G \to \infty$ the model (102) reduces to the classical neo-Hookean model

$$W(I_1) = \frac{1}{2}\mu(I_1 - 3), \tag{105}$$

for which $W_1 = \mu/2$ and $W_{11} = 0$, and the coefficients in appendix A simplify considerably.

5.1 Results

For the numerical solution of the system we use dimensionless quantities defined as

$$\hat{r} = \frac{r}{A},\ \ \hat{\alpha} = \alpha A,\ \ \hat{f}_\alpha(\hat{r}) = \frac{f_\alpha(r)}{A^2},\ \ \hat{g}_\alpha(\hat{r}) = \frac{g_\alpha(r)}{\sigma_{\mathrm{f}a}A},\ \ \hat{p}(\hat{r}) = \frac{p(r)}{\mu},\ \ \hat{\sigma}_{\mathrm{f}a} = \frac{\sigma_{\mathrm{f}a}}{\sqrt{\mu\varepsilon}}, \tag{106}$$

$$\begin{aligned} &\hat{y}_1(\hat{r}) = \hat{f}_\alpha(\hat{r}), \quad \hat{y}_2(\hat{r}) = \hat{f}'_\alpha(\hat{r}), \quad \hat{y}_3(\hat{r}) = \hat{f}''_\alpha(\hat{r}), \\ &\hat{y}_4(\hat{r}) = \hat{f}'''_\alpha(\hat{r}), \quad \hat{y}_5(\hat{r}) = \hat{g}_\alpha(\hat{r}), \quad \hat{y}_6(\hat{r}) = \hat{g}'_\alpha(\hat{r}), \end{aligned} \tag{107}$$

$$\hat{\boldsymbol{\mathcal{A}}}_0^* = \boldsymbol{\mathcal{A}}_0^*/\mu, \quad \hat{\mathbb{A}}_0^* = \varepsilon\mathbb{A}_0^*/\sigma_{\mathrm{f}a}, \quad \hat{\mathbf{A}}_0^* = \varepsilon\mathbf{A}_0^*, \tag{108}$$

and, as in [7], we use the specific value $G = 97.2$.

The non-dimensional system of equations now has the form $\hat{\mathbf{y}}' = \hat{\boldsymbol{\mathcal{M}}}\hat{\mathbf{y}}$, where $\hat{\boldsymbol{\mathcal{M}}}$, for the model (53), is given by (96) with M_{ij} replaced by the dimensionless $\hat{M}_{ij}$ defined by

$$\hat{M}_{41} = A^4M_{41}, \quad \hat{M}_{42} = A^3M_{42}, \quad \hat{M}_{43} = A^2M_{43}, \quad \hat{M}_{44} = AM_{44}, \tag{109}$$

$$\hat{M}_{62} = \frac{A^2M_{62}}{\sigma_{\mathrm{f}a}}, \quad \hat{M}_{63} = \frac{AM_{63}}{\sigma_{\mathrm{f}a}}, \quad \hat{M}_{64} = \frac{M_{62}}{\sigma_{\mathrm{f}a}}, \quad \hat{M}_{65} = A^2M_{65}, \quad \hat{M}_{66} = AM_{66}. \tag{110}$$

The corresponding non-dimensional forms of the boundary conditions are obtained from (98) by placing a 'hat' on each term with

$$\hat{b}_1 = \frac{Ab_1}{\mu}, \quad \hat{b}_2 = \frac{b_2}{\mu}, \quad \hat{b}_3 = \frac{b_3}{A\mu}, \quad \hat{b}_4 = \frac{b_4}{A^2\mu}, \quad \hat{b}_5 = \frac{b_5\sigma_{\mathrm{f}a}}{\mu}, \quad \hat{b}_6 = \frac{b_6\sigma_{\mathrm{f}a}}{A\mu}. \tag{111}$$

Solutions of the above system have been obtained using `NDSolve` in Mathematica [14], and we now illustrate the results for some specific values of the parameters involved.

5.1.1 Frequency results

First, with the values of $\hat{\sigma}_{\mathrm{f}a}$ that were used in [7] for the corresponding static bifurcation problem, the dimensionless squared frequency, as measured by $\rho\omega^2/\mu\alpha^2$ (denoted ζ for brevity), is plotted against λ_a in figure 1, with a different value of the pressure P given by (60) for each λ_a and $\hat{\sigma}_{\mathrm{f}a}$ pairing. In [7], for the same material model, the bifurcation curves were plotted with λ_a versus λ_z. The bifurcation results are recovered by setting $\omega = 0$. In particular, for $\lambda_z = 1.2$ the values of λ_a corresponding to bifurcation in figure 1 are the same as those that can be identified in the λ_a versus λ_z plots in [7]. The value $\hat{\sigma}_{\mathrm{f}a} = 0$ corresponds to the purely elastic case and application of a non-zero $\hat{\sigma}_{\mathrm{f}a}$ reduces the frequency for any given λ_a prior to the bifurcation value, which itself decreases as $\hat{\sigma}_{\mathrm{f}a}$ increases. If there is no pressure then the starting value of λ_a is slightly less than the 1 in figure 1 and is different for each $\hat{\sigma}_{\mathrm{f}a}$. For $\lambda_z = 1.2$, as in figure 1, for example, with $\hat{\sigma}_{\mathrm{f}a} = 0$ the minimum value of $\lambda_a = \lambda_z^{-1/2} \approx 0.913$.

Note that the dimensionless $\hat{\alpha} = \alpha A = 2n\pi A/(L\lambda_z)$ or $(2n+1)\pi A/(L\lambda_z)$ embodies different mode numbers n and aspect ratios A/L, so by fixing one and varying the other results for different mode numbers for a given aspect ratio or vice versa can be obtained. Indeed, by considering $\rho\omega^2A^2/\mu = \hat{\alpha}^2\zeta$ for given λ_z results for fixed A/L and different mode numbers n or for fixed mode number n and different A/L can be read off from the figure by multiplying the results therein by $\hat{\alpha}^2$. Thus, figure 1 captures these options compactly.

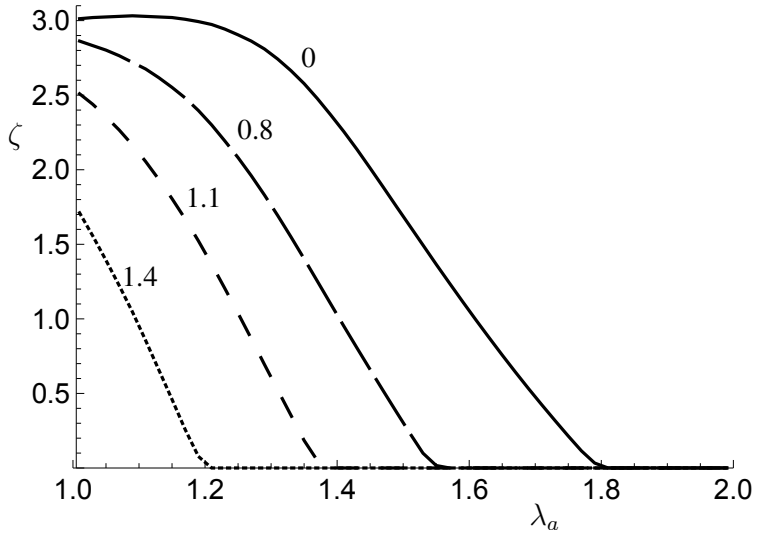

Figure 1: Plots of $\zeta = \rho\omega^2/\mu\alpha^2$ against λ_a for fixed $\lambda_z = 1.2$ with the values $0, 0.8, 1.1, 1.4$ of $\hat{\sigma}_{\mathrm{f}a}$ for a Gent electroelastic tube with $A/B = 0.85$, $L/B = 10$.

For $\hat{\sigma}_{\mathrm{f}a} = 0$ the result in figure 1 is consistent with that obtained in [15] for the purely elastic case where a rotating tube was considered (when specialized to the absence of rotation), although the parameters used and the method of presentation of the results were somewhat different.

To provide some interpretation of the results in figure 1 we refer to the corresponding plots in figure 2(a) of the dimensionless pressure $P^* = P/\mu$ versus λ_a for $\lambda_z = 1.2$ based on equation (60) with W_1 given by $(104)_1$, and the plots of λ_a versus λ_z in figure 2(b) obtained by setting $P = 0$ (the latter are the same curves as provided in [7], the pressure being positive above the curve for each relevant value of $\hat{\sigma}_{\mathrm{f}a}$). For $\hat{\sigma}_{\mathrm{f}a} = 0$, as λ_a increases from its minimum value where $P = 0$ bifurcation becomes possible when λ_a reaches the approximate value 1.8, and P is positive within this range. For $\hat{\sigma}_{\mathrm{f}a} = 0.8$, P is positive for λ_a greater than approximately 1.1 up to the approximate value 1.55 where bifurcation becomes possible.

However, for real values of the frequency for $\hat{\sigma}_{\mathrm{f}a}$ greater than approximately 1.1 a negative pressure is required, equivalently an external pressure. This is even more evident for larger values of $\hat{\sigma}_{\mathrm{f}a}$. For example, for $\hat{\sigma}_{\mathrm{f}a} = 1.4$ a negative value of P is required for the existence of a real frequency up to the approximate bifurcation value of $\lambda_a = 1.2$ (P is positive only for λ_a greater than approximately 1.55).

We now recall that $\sigma_{\mathrm{f}a} = Q/(2\pi AL\lambda_a\lambda_z)$, which depends on the deformation since Q is a constant. Thus, it makes sense to use a dimensionless form of Q instead of $\hat{\sigma}_{\mathrm{f}a}$ in representing the results. An appropriate non-dimensionalization of Q, denoted $\hat{Q}$, is defined by

$$\hat{Q} = \frac{Q}{2\pi AL\sqrt{\mu\varepsilon}} = \lambda_a\lambda_z\hat{\sigma}_{\mathrm{f}a}. \tag{112}$$

Results for fixed $\hat{Q}$ are shown in figure 3(a) and can be obtained from those for $\hat{\sigma}_{\mathrm{f}a}$ in figure 1 on use of (112). The general character is the same as in figure 1 but the bifurcation values of λ_a (on the horizontal axis) are different because of the dependence of $\hat{\sigma}_{\mathrm{f}a}$ on λ_a. Corresponding results for $\lambda_z = 0.9$ are shown in figure 3(b) for comparison. In this case when the pressure

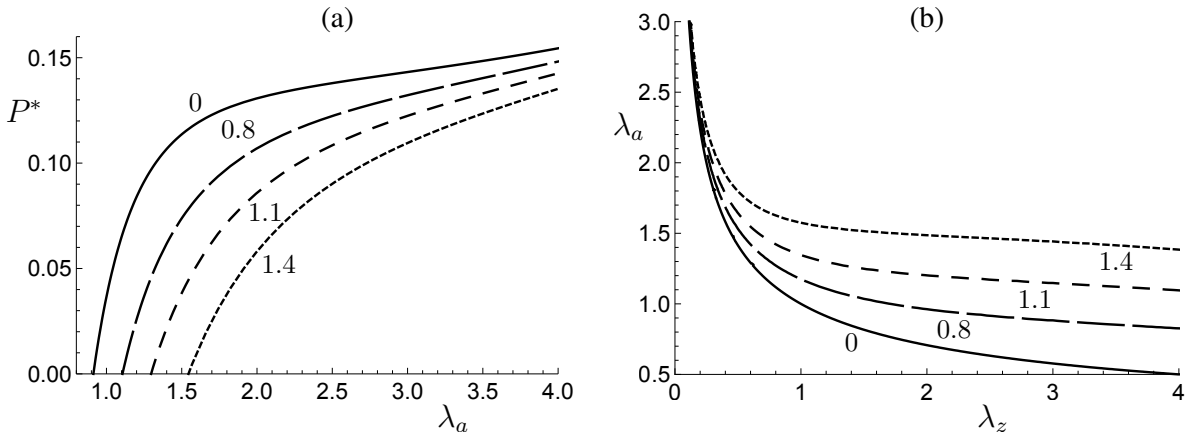

Figure 2: Plots of: (a) $P^* = P/\mu$ against λ_a for fixed $\lambda_z = 1.2$; (b) λ_a versus λ_z for $P = 0$, in each case for $\hat{\sigma}_{\mathrm{f}a} = 0, 0.8, 1.1, 1.4$ for a Gent electroelastic tube with $A/B = 0.85$, $L/B = 10$ based on equation (60).

is zero the starting value of λ_a is approximately 1.05, smaller values would require negative pressure, but the general character of the results is the same as for $\lambda_z = 1.2$.

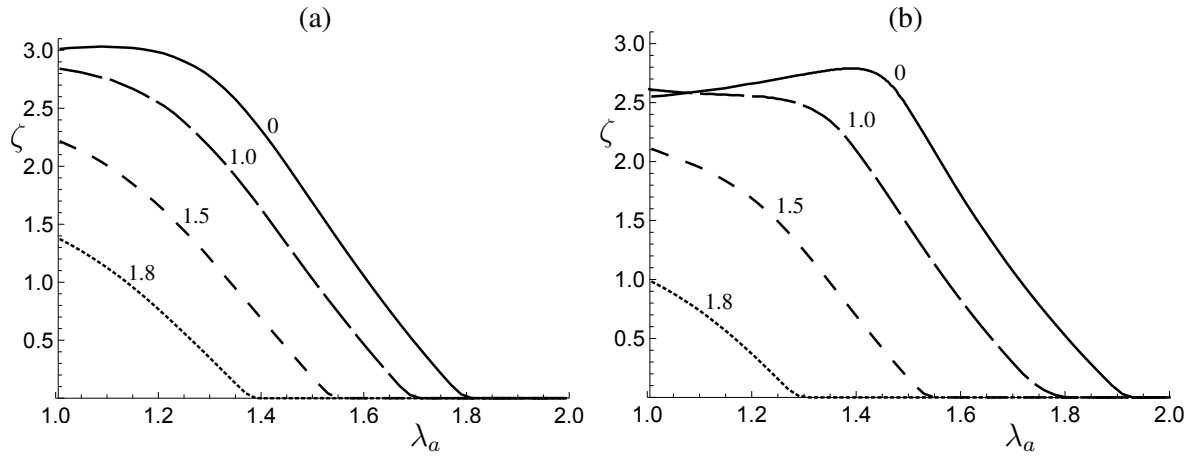

Figure 3: Plots of $\zeta = \rho\omega^2/\mu\alpha^2$ against λ_a for fixed $\lambda_z = 1.2$ (a) and $\lambda_z = 0.9$ (b) with the values $0, 1, 1.5, 1.8$ of $\hat{Q}$ for a Gent electroelastic tube with $A/B = 0.85$, $L/B = 10$.

The connection (57) between the potential difference V and Q is now put in dimensionless form as

$$\hat{V} = \frac{V\sqrt{\varepsilon}}{A\sqrt{\mu}} = \frac{\hat{Q}}{\lambda_z}\log(b/a) = \frac{\hat{Q}}{2\lambda_z}\log[1 + \lambda_z^{-1}\lambda_a^{-2}(B^2/A^2 - 1)]. \tag{113}$$

This connection can be used to determine the dependence of $\rho\omega^2/\mu\alpha^2$ on fixed values of $\hat{V}$. The results are shown in figure 4, for both $\lambda_z = 1.2$ and $\lambda_z = 0.9$. The values of $\hat{V}$ do not correspond directly with those of $\hat{Q}$ in figure 3 because of the dependence on λ_a in (113).

In parallel with figure 2, figure 5 illustrates the dependence of P^* on λ_a for $\lambda_z = 1.2$ and plots of λ_a versus λ_z corresponding to $P = 0$ for several values of $\hat{V}$, somewhat different values than in figure 4 to avoid the curves disappearing off the scale for the larger values of $\hat{V}$

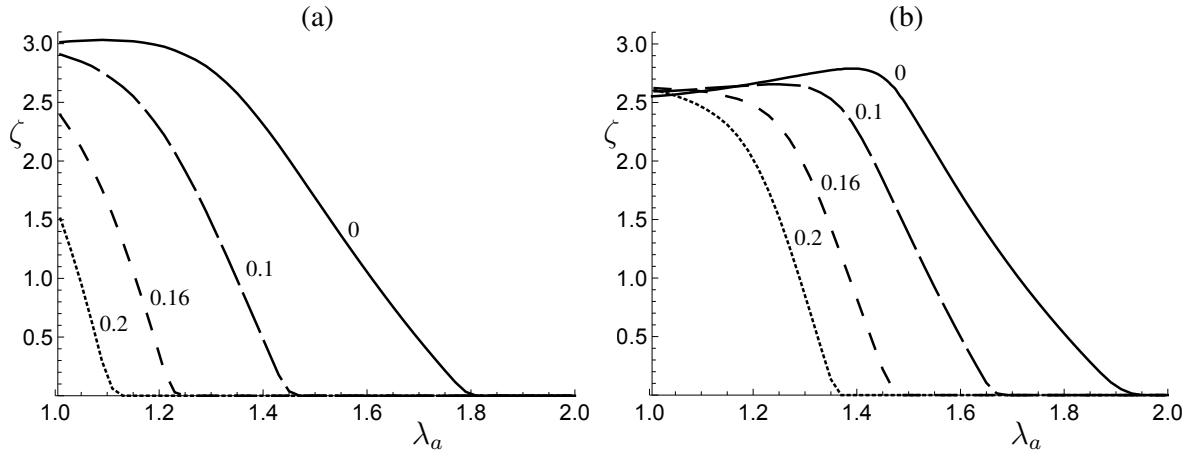

Figure 4: Plots of $\rho\omega^2/\mu\alpha^2$ against λ_a for fixed $\lambda_z = 1.2$ (a) and $\lambda_z = 0.9$ (b) with the values $0, 0.1, 0.16, 0.2$ of $\hat{V}$ for a Gent electroelastic tube with $A/B = 0.85$, $L/B = 10$.

used in figure 4. The characters of the P^* plots in figures 2(a) and 5(a) are similar except that, for larger values of λ_a, P^* tends to the same asymptotic value for each $\hat{\sigma}_{\rm fa}$, but different limits for the different values of $\hat{V}$. By contrast, the results for $P = 0$ in figure 2(b) are markedly different from those in figure 5(b). In particular, they indicate that a negative pressure is needed for the existence of real frequencies (including zero, corresponding to static bifurcation).

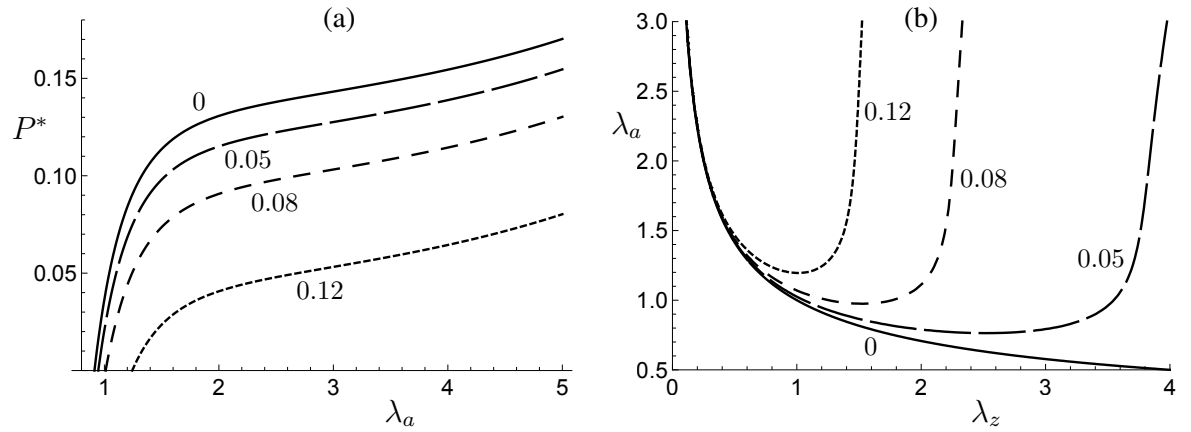

Figure 5: Plots of (a) $P^* = P/\mu$ against λ_a for fixed $\lambda_z = 1.2$ and (b) λ_a versus λ_z for $P = 0$, in each case with the values $0, 0.05, 0.08, 0.12$ of $\hat{V}$ for a Gent electroelastic tube with $A/B = 0.85$, $L/B = 10$.

An alternative perspective is obtained by considering the dependence of $\rho\omega^2 A^2/\mu$, denoted ξ, on the (dimensionless) wave number $\hat{\alpha}$ for fixed values of λ_a as well as λ_z. To illustrate this we refer to figure 6 where ξ is plotted against $\hat{\alpha}$ for several values of $\hat{Q}$ in (a) and several values of $\hat{V}$ in (b), and for a small range of values of $\hat{\alpha}$. For fixed λ_a and λ_z the values of $\hat{V}$ are proportional to those of $\hat{Q}$, according to equation (113) with $\hat{Q} = 0, 1, 1.5, 1.8$ in figure 6(a) translating to $\hat{V} = 0, 0.84, 0.13, 0.15$, which are different from the values used in figure 6(b). Note, in particular, that for $\hat{V} = 0.2$ there is no real frequency ($\lambda_a = 1.2$ is outside the existence range shown in figure 4(a) in this case).

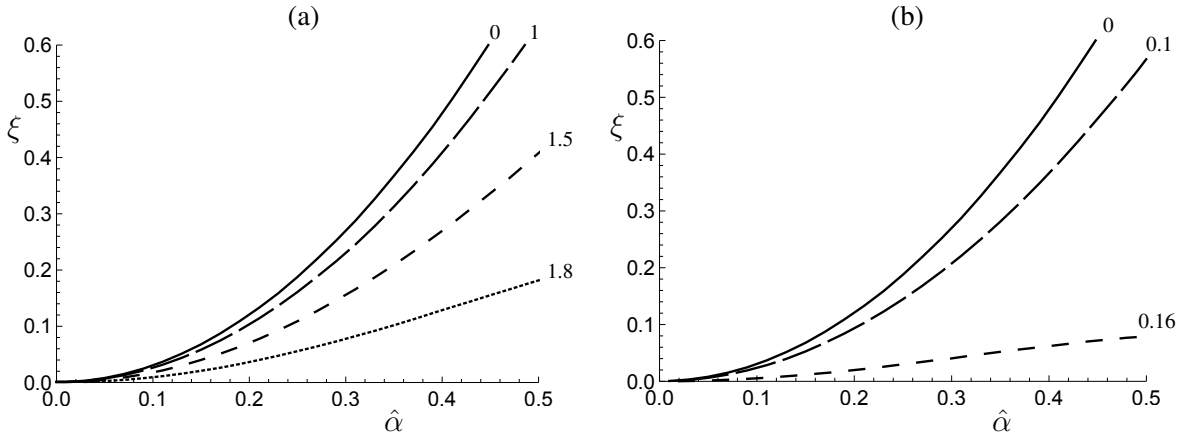

Figure 6: Plots of $\xi = \rho\omega^2 A^2/\mu$ versus $\hat{\alpha}$ for $\lambda_a = \lambda_z = 1.2$: (a) $\hat{Q} = 0, 1, 1.5, 1.8$; (b) $\hat{V} = 0, 0.1, 0.16, 0.2$ for a Gent electroelastic tube with $A/B = 0.85$, $L/B = 10$.

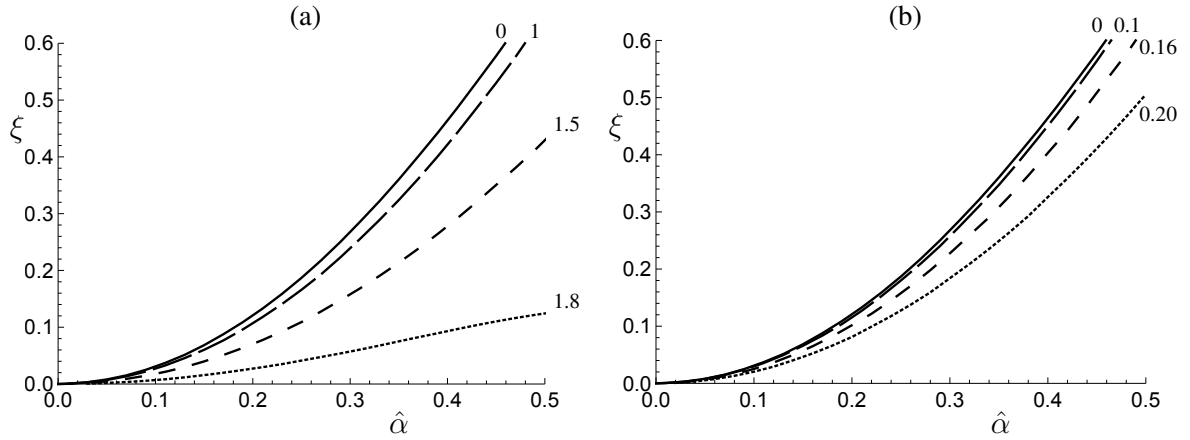

Figure 7: Plots of $\xi = \rho\omega^2 A^2/\mu$ versus $\hat{\alpha}$ for $\lambda_a = 1.2, \lambda_z = 0.9$: (a) $\hat{Q} = 0, 1, 1.5, 1.8$; (b) $\hat{V} = 0, 0.1, 0.16, 0.2$ for a Gent electroelastic tube with $A/B = 0.85$, $L/B = 10$.

The counterpart of figure 6 for $\lambda_a = 1.2, \lambda_z = 0.9$ is shown in figure 7. In this case the frequency does exist for $\hat{V} = 0.2$. Note that for fixed $\hat{Q}$ there is very little difference between the results for the different values of λ_z, in contrast to the situation for fixed $\hat{V}$.

Now let us look in more detail at an expanded version of figure 6(b), for a slightly larger range of values of $\hat{\alpha}$, as shown in figure 8(a). In this example second modes also arise and these are also included (dashed curves), although the main interest is in the fundamental mode. For the model and range of parameters used here no other modes have been found. As in figure 6(b) there is no real frequency for $\hat{V} = 0.2$, while the result for $\hat{V} = 0.16$ shows that there is no real (fundamental mode) frequency for a critical value (≈ 0.85) of $\hat{\alpha}$ in figure 8(a) which is beyond the values shown in figure 6(b). This prompts the question as to what happens to the fundamental modes for even larger values of $\hat{\alpha}$, and figure 8(b) exemplifies this. For small values of $\hat{V}$ frequencies exist for all $\hat{\alpha}$, but as $\hat{V}$ increases there are no real frequencies beyond a $\hat{V}$-dependent critical value of $\hat{\alpha}$, which is the case for $\hat{V} = 0.14$, for example.

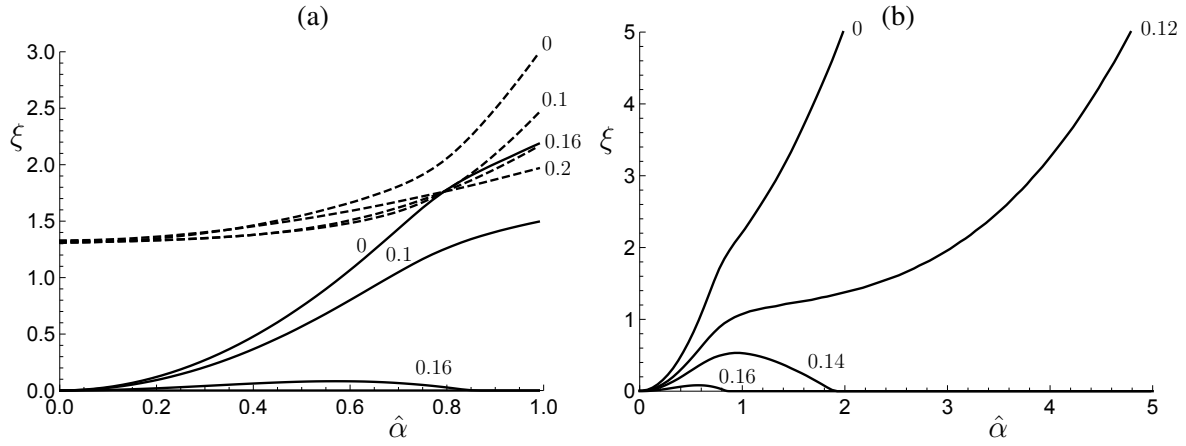

Figure 8: Plots of $\xi = \rho\omega^2 A^2/\mu$ versus $\hat{\alpha}$ for a Gent electroelastic tube with $A/B = 0.85$, $L/B = 10$ and $\lambda_a = \lambda_z = 1.2$: (a) plots of the fundamental mode (continuous curves) and second modes (dashed curves) for $\hat{V} = 0, 0.1, 0.16, 0.2$; (b) plots of the fundamental mode for $\hat{V} = 0, 0.12, 0.14, 0.16$.

5.1.2 Wave speed results

Instead of vibrations with fixed incremental end conditions we now consider the propagation of waves, again with a fixed value of the axial stretch but with the incremental displacement and stress allowed to adjust as the wave propagates. In this case α is the wave number without a specified value related to end conditions. The wave speed, denoted v, is given by $v = \omega/\alpha$. The governing equations, and the boundary conditions on $r = a$ and $r = b$, are unchanged and v is therefore determined by the preceding formula. In figure 9 the dimensionless squared wave speed $\rho v^2/\mu$, denoted ς, is plotted against $\hat{\alpha}$ for several values of $\hat{Q}$ and $\hat{V}$ in figures 9(a) and (b), respectively, with $\lambda_a = \lambda_z = 1.2$. Note, in particular, that for the larger values of $\hat{Q}$ and $\hat{V}$ there is no real wave speed beyond a critical value of $\hat{\alpha}$, which is zero in some cases, for example for $\hat{V} = 0.2$.

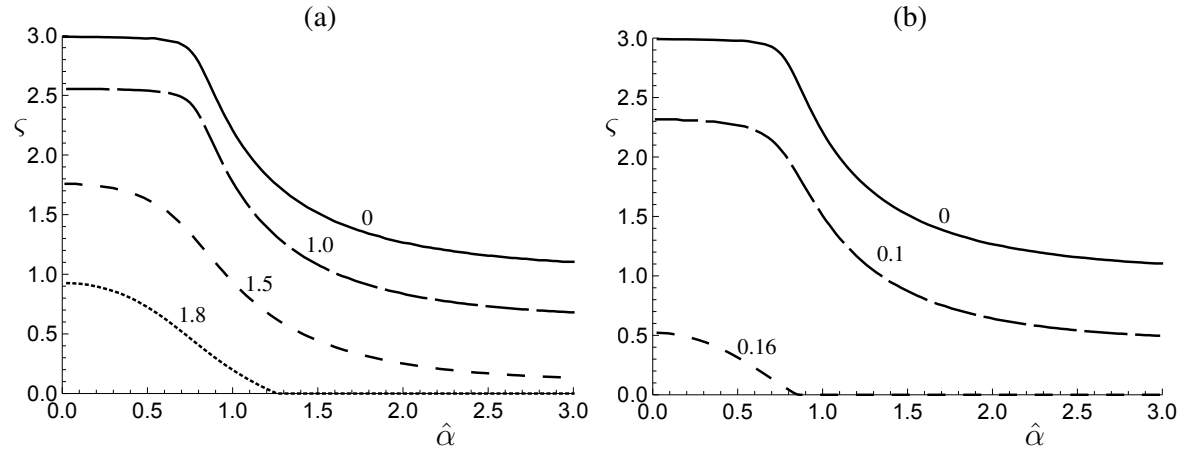

Figure 9: Plots of $\varsigma = \rho v^2/\mu$ against $\hat{\alpha}$ for a Gent electroelastic tube with $A/B = 0.85$, $L/B = 10$ and $\lambda_a = \lambda_z = 1.2$: (a) for $\hat{Q} = 0, 1, 1.5, 1.8$; (b) for $\hat{V} = 0, 0.1, 0.16$.

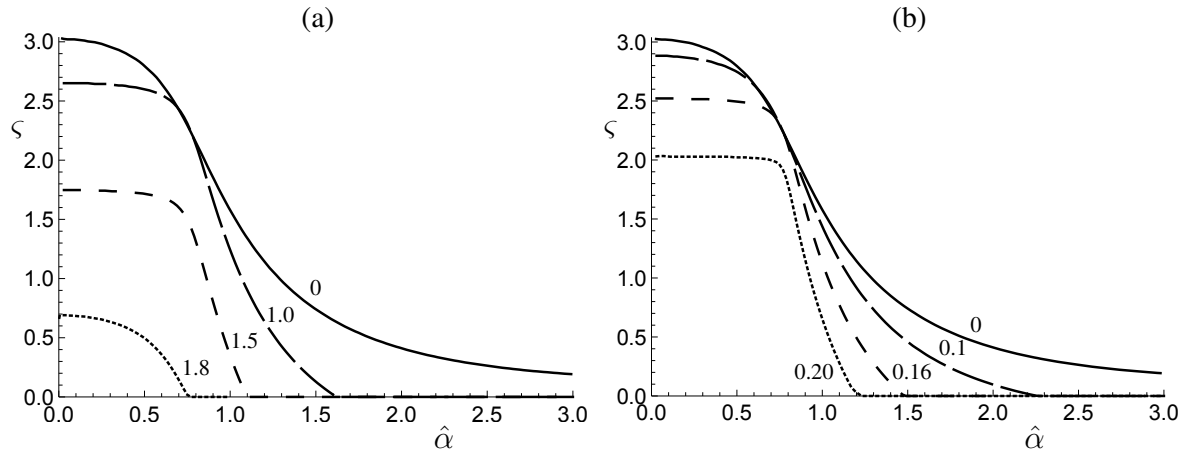

Figure 10: Plots of $\varsigma = \rho v^2/\mu$ against $\hat{\alpha}$ for a Gent electroelastic tube with $A/B = 0.85$, $L/B = 10$ and $\lambda_a = 1.2, \lambda_z = 0.9$: (a) for $\hat{Q} = 0, 1, 1.5, 1.8$; (b) for $\hat{V} = 0, 0.1, 0.16, 0.2$.

Corresponding results are shown in figure 10 with $\lambda_z = 1.2$ replaced by $\lambda_z = 0.9$ to illustrate the dependence on the axial stretch. In this case waves do exist for $\hat{V} = 0.2$ for small values of $\hat{\alpha}$, and the cut-off values of $\hat{\alpha}$ are reduced, so that the range of values of the wave number for which the underlying configuration is stable is likewise reduced.

5.1.3 Neo-Hookean results

In Shmuel & deBotton [10] the propagation of incremental axisymmetric waves in a tube was examined for a neo-Hookean electroelastic model. However, the incremental problem considered therein is somewhat different from that examined here in that neither the incremental potential difference nor charge was specified on the electrodes, so that a field exterior to the tube was incorporated into their analysis. Here, by contrast, no exterior field is generated when the incremental voltage (or charge) is specified on the electrodes. We therefore present some results for the neo-Hookean model in order to provide a qualitative comparison of the two approaches. In [10] neither an internal nor an external pressure was included, so we confine our results to the case $P = 0$. They considered three different tube thicknesses, the thinnest of which was for $A/B \approx 0.91$, which is the closest to our value of 0.85 and therefore provides a reasonable basis for comparison. They also used $L/B = 10$.

In figure 11 results are presented for the fundamental mode as $\xi = \rho\omega^2 A^2/\mu$ versus $\hat{\alpha}$ for several values of $\hat{V}$ with $A/B = 0.85$, $L/B = 10$, $\lambda_z = 1.2$ and $P = 0$. The counterparts of figure 11 in [10] involved, in the present notation, plots of $\sqrt{\xi}H/A$ against $\hat{\alpha}H/A$, where $H = B - A$ is the reference thickness of the tube. The relevant figures in [10] are 4(d) and 5(d), in which, as well as different scales, a different non-dimensionalization of the potential difference was used, corresponding to $\hat{V}A/H$ (their $A/H = 10$). Here we use $\lambda_z = 1.2$, whereas the nearest values of λ_z in [10] were 1 and 2, but the character of the results for these two values was similar. Thus, our results for $\lambda_z = 1.2$ provide a meaningful qualitative comparison/contrast with those in [10] rather than a precise numerical one.

Figure 11(a) shows the typical features of our results, with further elaboration in figure 11(b) for the larger values of $\hat{V}$, for which there is a finite cut-off band within which there is no real frequency. These are quite different from the results in [10], although for lower values

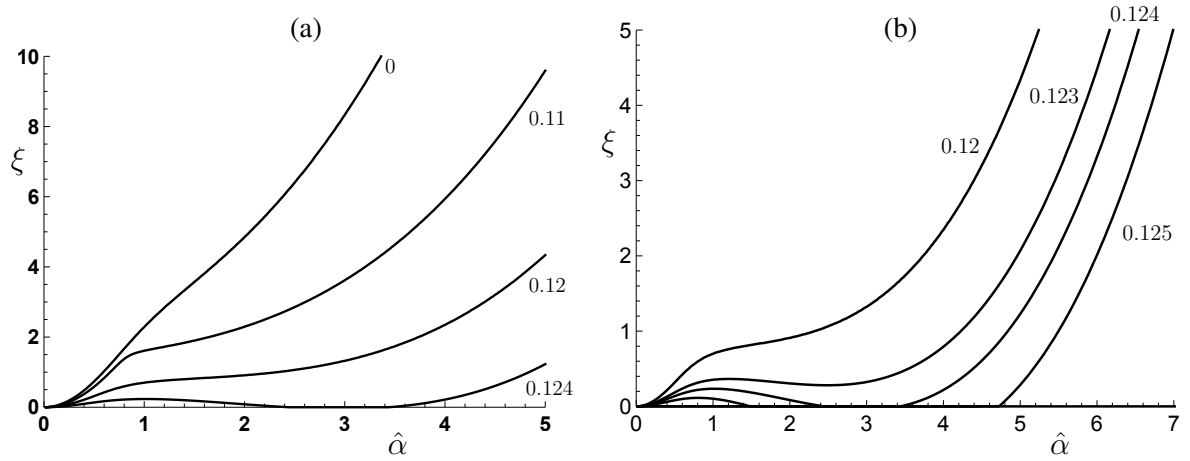

Figure 11: Plots of $\xi = \rho\omega^2 A^2/\mu$ against $\hat{\alpha}$ for a neo-Hookean electroelastic tube with $A/B = 0.85$, $L/B = 10$ and $\lambda_z = 1.2$ with $P = 0$ (fundamental mode): (a) for $\hat{V} = 0, 0.11, 0.12, 0.124$; (b) for $\hat{V} = 0.12, 0.123, 0.124, 0.125$.

of $\hat{V}$ there are some similarities, in particular the evident monotonicity. For even larger values of $\hat{V}$, for example for $\hat{V} = 0.133$ and 0.14 there is no real frequency, at least for values of $\hat{\alpha} \in [0, 10]$.

Although results were not given in [10] for the second mode, for completeness in figure 12 we provide some results for the second mode. A feature here is that for larger values of $\hat{V}$ there is a cut-off value of $\hat{\alpha}$ beyond which there is no real frequency.

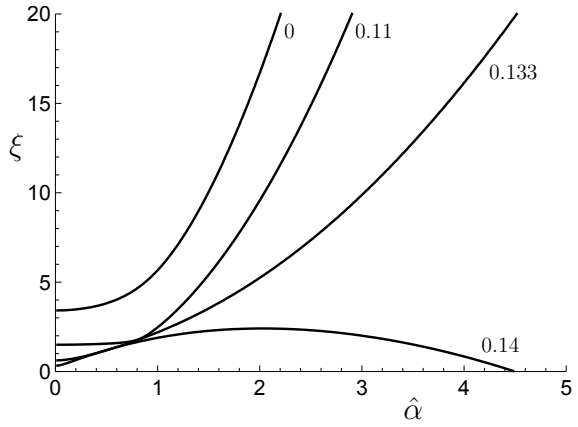

Figure 12: Plots of $\xi = \rho\omega^2 A^2/\mu$ against $\hat{\alpha}$ for a neo-Hookean electroelastic tube with $A/B = 0.85$, $L/B = 10$ and $\lambda_z = 1.2$ with $P = 0$ (second mode): $\hat{V} = 0, 0.11, 0.133, 0.14$.

6 Concluding discussion

In the present paper we have examined both axisymmetric vibrations and the propagation of axisymmetric waves in a circular cylindrical Gent electroelastic model tube following a general formulation of the governing equations and boundary conditions based on the general theory

of isotropic nonlinear electroelasticity. The results highlight the dependence of the frequency of vibration and wave speed on the tube geometry, applied deformation and electric field. In particular, the bifurcation results obtained previously in [7] are recovered as a special case when the frequency vanishes. Results are also illustrated for a neo-Hookean electroelastic model and compared with those obtained in [10]. There are some similarities but also some significant differences in the outcomes for the different incremental boundary conditions adopted here and in [10], in particular related to cut-off frequencies. The results for the Gent and neo-Hookean models results are broadly similar, although, unlike for the neo-Hookean model, for the Gent model there is no real frequency for higher values of $\hat{\alpha}$ beyond the cut-off values, as can be seen by comparing figure 8(b) with figure 11(b).

Appendices

A Evaluation of terms in the governing equations

We obtain from the formula $\lambda = r/R$, equation (49), $\lambda_r = \lambda^{-1}\lambda_z^{-1}$ and $(51)_1$

$$r\lambda_r' = \lambda_r(\lambda^2\lambda_z - 1), \quad r\lambda' = -\lambda(\lambda^2\lambda_z - 1), \quad rI_1' = -2\lambda_r^2(\lambda^2\lambda_z - 1)^2(\lambda^2\lambda_z + 1),$$

on use of which with rD constant giving $rD' = -D$ we obtain

$$\begin{aligned}
r^2\tau_{rr}'' =& -4W_{11}\lambda_r^4(\lambda^2\lambda_z - 1)(\lambda^4\lambda_z^2 - 1)^2 - 2W_1\lambda_r^2(\lambda^2\lambda_z - 1)(2\lambda^4\lambda_z^2 + \lambda^2\lambda_z + 3) + 3dD,\\
rc' =& -4W_{11}\lambda_r^4(\lambda^2\lambda_z - 1)^2(\lambda^2\lambda_z + 1) + 4W_1\lambda_r^2(\lambda^2\lambda_z - 1) - 2dD,\\
r^2c'' =& \, 8W_{111}\lambda_r^6(\lambda^2\lambda_z - 1)^4(\lambda^2\lambda_z + 1)^2 + 4W_{11}\lambda_r^4(\lambda^2\lambda_z - 1)^2(3\lambda^2\lambda_z + 7)\\
& -12W_1\lambda_r^2(\lambda^2\lambda_z - 1) + 6dD,\\
rb' =& -4W_{111}\lambda_r^6(\lambda^2\lambda_z - 1)^2(\lambda^2\lambda_z + 1)(\lambda^2\lambda_z^4 - 1)^2\\
& -2W_{11}\lambda_r^4(\lambda^2\lambda_z - 1)(\lambda^6\lambda_z^6 + \lambda^4\lambda_z^2 + 3\lambda^2\lambda_z^4 - 5) + 2W_1\lambda_r^2(\lambda^2\lambda_z - 1) - dD,\\
rk' =& -8W_{111}\lambda_r^6(\lambda^2\lambda_z - 1)(\lambda^4\lambda_z^2 - 1)^2(\lambda^2\lambda_z^4 - 1)\\
& -4W_{11}\lambda_r^4(\lambda^2\lambda_z - 1)(2\lambda^6\lambda_z^6 + \lambda^4\lambda_z^2 + 2\lambda^2\lambda_z^4 - 5) + 4W_1\lambda_r^2(\lambda^2\lambda_z - 1) - 2dD.
\end{aligned}$$

B Components of the matrix $\mathcal{M}$

The components $M_{41}, M_{42}, M_{43}, M_{44}$ in (96) are given by

$$\begin{aligned}
M_{41} &= -\alpha^2[2\alpha^2r^2W_1\lambda_z^2 - \rho\omega^2r^2 + 2A]/(2r^2W_1\lambda_r^2),\\
M_{42} &= -[2\alpha^2r^2B - \rho\omega^2r^2 - 2C]/(2r^3W_1\lambda_r^2),
\end{aligned}$$

where

$$
\begin{aligned}
A &= -4W_{111}\lambda_r^6(\lambda^2\lambda_z-1)^3(\lambda^2\lambda_z+1)^2\lambda^2\lambda_z(\lambda_z^3-1)\\
&\quad +2W_{11}\lambda_r^4(\lambda^2\lambda_z-1)(\lambda^6\lambda_z^3+\lambda^4\lambda_z^2-2\lambda^4\lambda_z^5-2\lambda^2\lambda_z^4+\lambda^2\lambda_z-4\lambda_z^3+5)\lambda^2\lambda_z\\
&\quad +2W_1\lambda_r^2(\lambda^2\lambda_z-1)(\lambda^2\lambda_z+1)\lambda^2\lambda_z,\\
B &= 4W_{111}\lambda_r^6(\lambda^2\lambda_z-1)^2(\lambda^2\lambda_z+1)(\lambda_z^4\lambda^2-1)^2\\
&\quad +2W_{11}\lambda_r^4[(\lambda^2\lambda_z^4-1)^2+(\lambda^2\lambda_z-1)^2(\lambda^2\lambda_z+1)(\lambda_z^4\lambda^2+1)+4(\lambda^2\lambda_z-1)(\lambda^2\lambda_z^4-1)]\\
&\quad +W_1\lambda_r^2(\lambda_z^4\lambda^2-2\lambda_z\lambda^2+3),\\
C &= 4W_{111}\lambda_r^6(\lambda^2\lambda_z-1)^4(\lambda^2\lambda_z+1)^2+4W_{11}\lambda_r^4(\lambda^2\lambda_z-1)^2(3\lambda^2\lambda_z+5)\\
&\quad -3W_1\lambda_r^2(4\lambda^2\lambda_z-5),
\end{aligned}
$$

$$
\begin{aligned}
M_{43} &= \{\alpha^2r^2[4W_{11}\lambda_r^4(\lambda^2\lambda_z^4-1)^2+2W_1\lambda_r^2(\lambda_z^4\lambda^2+1)]-2C-\rho\omega^2r^2\}/(2r^2W_1\lambda_r^2),\\
M_{44} &= [4W_{11}\lambda_r^4(\lambda^2\lambda_z-1)^2(\lambda^2\lambda_z+1)-2W_1\lambda_r^2(2\lambda^2\lambda_z-3)]/(rW_1\lambda_r^2).
\end{aligned}
$$

References

[1] Zhu J, Stoyanov H, Kofod G, Suo Z. 2010 Large deformation and electromechanical instability of a dielectric elastomer tube actuator. *J. Appl. Phys.* **108**, 074113.

[2] Melnikov A, Ogden RW. 2016 Finite deformations of an electroelastic circular cylindrical tube. *Z. Angew. Math. Phys.* **67**, 140.

[3] Dorfmann L, Ogden RW. 2014 Instabilities of an electroelastic plate. *Int. J. Eng. Sci.* **77**, 79–101.

[4] Melnikov A, Ogden RW. 2018 Bifurcation of finitely deformed thick-walled electroelastic cylindrical tubes subject to a radial electric field. *Z. Angew. Math. Phys.* **69**, 60.

[5] Dorfmann A, Ogden RW. 2010 Nonlinear electroelasticity: incremental equations and stability. *Int. J. Eng. Sci.* **48**, 1–14.

[6] Dorfmann L, Ogden RW. 2014 *Nonlinear theory of electroelastic and magnetoelastic interactions*. New York: Springer.

[7] Dorfmann A, Ogden RW. 2019. Instabilities of soft dielectrics. *Phil. Trans. R. Soc. A* **377**, 20180077

[8] Su Y, Zhou W, Chen W, Lü C. 2016 On buckling of a soft incompressible electroactive hollow cylinder. *Int. J. Solids Struct.* **97–98**, 400–416.

[9] Dorfmann A, Ogden RW. 2010 Electroelastic waves in a finitely deformed electroactive material. *IMA J. Appl. Math.* **75**, 603–636.

[10] Shmuel G, deBotton G. 2013 Axisymmetric wave propagation in finitely deformed dielectric elastomer tubes. *Proc. R. Soc. Lond. A* **469**, 20130071.

[11] Ogden RW. 1972 Large deformation isotropic elasticity – on the correlation of theory and experiment for incompressible rubberlike solids. *Proc. R. Soc. Lond. A* **326**, 565–584.

[12] Dorfmann A, Ogden RW. 2005 Nonlinear electroelasticity. *Acta Mech.* **174**, 167–183.

[13] Gent AN. 1996 A new constitutive relation for rubber. *Rubber Chem. Technol.* **69**, 59–61.

[14] Wolfram Research Inc., Mathematica 11.3, Champaign, IL, 2018.

[15] Haughton DM. 1984 Wave speeds in rotating thick-walled elastic tubes. *J. Sound Vib.* **97**, 107–116.